Inorganic Chemistry

pubs.acs.org/IC

Viewpoint

Using Reduction Kinetics to Control and Predict the Outcome of a Colloidal Synthesis of Noble-Metal Nanocrystals

Quynh N. Nguyen,[†] Ruhui Chen,[†] Zhiheng Lyu,[†] and Younan Xia*

Cite This: *Inorg. Chem.* 2021, 60, 4182–4197

Read Online

ACCESS | Metrics & More | Article Recommendations

ABSTRACT: Improving the performance of noble-metal nanocrystals in various applications critically depends on our ability to manipulate their synthesis in a rational, robust, and controllable fashion. Different from a conventional trial-and-error approach, the reduction kinetics of a colloidal synthesis has recently been demonstrated as a reliable knob for controlling the synthesis of noble-metal nanocrystals in a deterministic and predictable manner. Here we present a brief Viewpoint on the recent progress in leveraging reduction kinetics for controlling and predicting the outcome of a synthesis of noble-metal nanocrystals. With a focus on Pd nanocrystals, we first offer a discussion on the correlation between the initial reduction rate and the internal structure of the resultant seeds. The kinetic approaches for controlling both nucleation and growth in a one-pot setting are then introduced with an emphasis on manipulation of the reduction pathways taken by the precursor. We then illustrate how to extend the strategy into a bimetallic system for the preparation of nanocrystals with different shapes and elemental distributions. Finally, the influence of speciation of the precursor on reduction kinetics is highlighted, followed by our perspectives on the challenges and future endeavors in achieving a controllable and predictable synthesis of noble-metal nanocrystals.

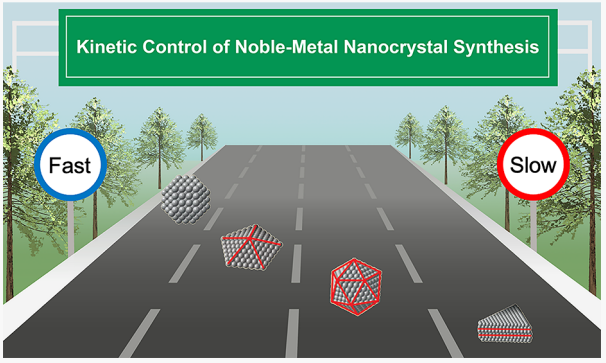

1. INTRODUCTION

Noble-metal nanocrystals have received ever-increasing attention owing to their excellent merits for fundamental studies and broad applications ranging from electronics[1,2] to photonics,[3,4] catalysis,[5−7] and biomedicine.[8−10] In addition to the novel features arising from size reduction, the properties of noble-metal nanocrystals are strongly dependent on their geometric shapes.[11] A notable example can be found in heterogeneous catalysis, where the activity and/or selectivity of a catalyst based upon noble-metal nanocrystals can be optimized by engineering the shape and thus arrangement of atoms on the surface.[7,12−14] In the case of Pd nanocrystals for formic acid oxidation, the specific activity of cubes enclosed by {100} facets shows a 2-fold enhancement relative to that of the {111}-terminated tetrahedral counterparts, whereas right bipyramids exhibit further enhanced activity compared to cubes due to the larger specific surface area and the presence of a twin plane.[15] In the case of Pt catalysts for the hydrogenation of benzene, cubic nanocrystals encased by {100} facets yielded cyclohexene as the only product, while both cyclohexane and cyclohexene were produced on cuboctahedral nanocrystals covered by a mixture of {111} and {100} facets.[16,17] It should be noted that there are also arguments on whether shape-controlled nanocrystals have a real impact on industrial catalysis because shape deformation, such as dissolution of atoms and intra- and interparticle sintering, might be observed during a catalytic process, which is detrimental to the performance of catalysts in most cases.[18,19] To this end, the degrading performance of nanocrystals losing shape and structure under harsh environments, in turn, attests to the importance of controlling and maintaining the shape of nanocrystals in catalysis. In understanding and optimizing the performance of noble-metal nanocrystals in catalysis and related applications, it is highly desirable to develop new methods for the facile, robust, and predictable synthesis of nanocrystals with diverse but well-defined shapes.

Thanks to the improved understanding of nucleation and growth mechanisms, the past two decades have witnessed the successful syntheses of noble-metal nanocrystals with a myriad of shapes and structures (Figure 1).[7,11,20−22] Among the different synthetic methodologies, colloidal synthesis in a solution phase has proven to be the most reproducible, versatile, and popular route. In a typical synthesis, metal atoms, which are the building blocks of nanocrystals, can be generated

Special Issue: Inorganic Chemistry of Nanoparticles

Received: December 7, 2020
Published: February 1, 2021

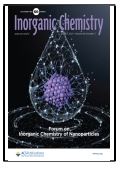

https://dx.doi.org/10.1021/acs.inorgchem.0c03576
Inorg. Chem. 2021, 60, 4182–4197

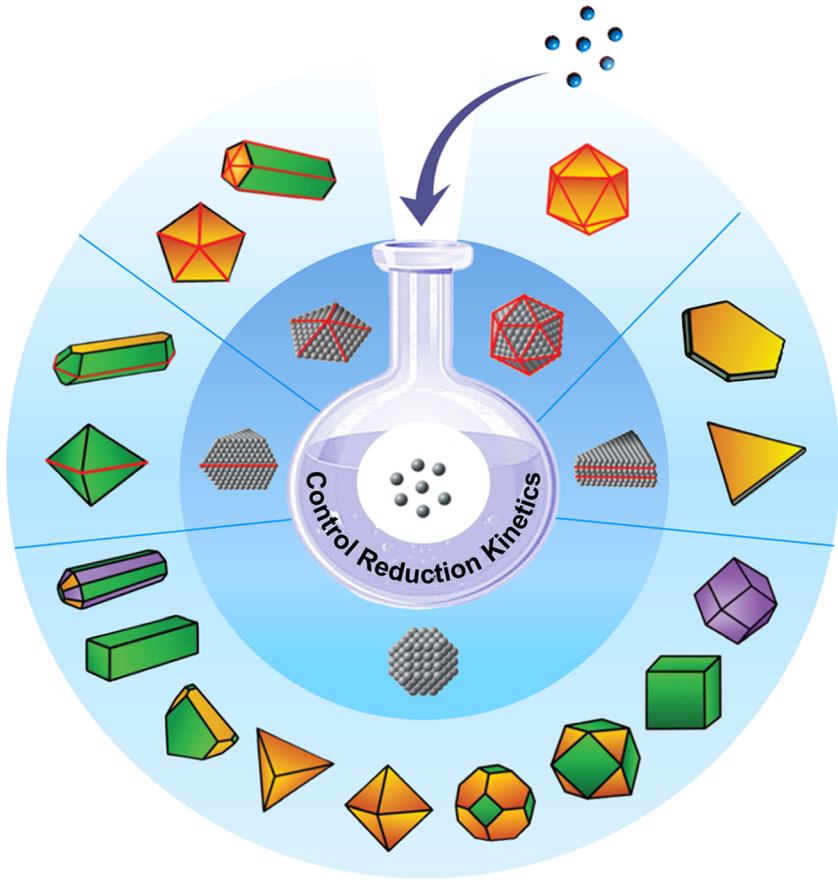

Figure 1. Schematic illustration showing the correlation between the internal structures of the seeds and the shapes of the final products. The metal atoms (in the center) are formed via the reduction or decomposition of a precursor (on the top), followed by their aggregation into nuclei, evolution into five major types of seeds (in the middle ring), and then growth to nanocrystals with distinct shapes (in the outer ring). The red lines indicate the twin defects or stacking faults, while the green, purple, and yellow colors indicate the {100}, {110}, and {111} facets on a nanocrystal, respectively. Adapted with permission from ref 25. Copyright 2017 Royal Society of Chemistry.

via either reduction or decomposition of a precursor.[23] As described by the LaMer model, once the concentration of atoms reaches the threshold for nucleation, nuclei will be formed through random aggregation,[24] followed by their evolution into crystalline seeds with well-defined internal structures (the middle ring in Figure 1).[25] The as-formed seeds subsequently grow into larger nanocrystals with distinct shapes, as governed by their internal structure and the interplay between thermodynamic (e.g., surface capping) and kinetic (e.g., reduction rate) parameters (the outer ring in Figure 1).[26−28] With the advancement of instrumentation in recent years, nonclassical nucleation pathways such as cluster-[29−31] or amorphous-phase-mediated[32] crystallization have also been proposed and validated in certain instances. Considering the debatable generality of these mechanisms, the direct involvement of reduction by an electron beam in these studies, and the complexity in kinetic analysis of non-classical nucleation, classical nucleation theory still serves as the focus of this Viewpoint. Although there is no one-to-one correspondence, the geometric shape taken by the nanocrystal has a clear correlation with the internal structure of the seed involved. To ensure the formation of nanocrystals with a particular shape, it is necessary to obtain the seed featuring the right internal structure during the nucleation process.

Despite significant progress, most of the synthetic protocols developed so far largely relied on a trial-and-error approach. A quantitative understanding of the driving forces underlying the nucleation and growth pathways would provide a powerful route to the rational and reproducible production of noble-metal nanocrystals with desired shapes and properties. Recent studies have demonstrated that the reduction kinetics of the precursor plays an essential role in controlling not only the internal structures of the seeds but also their growth patterns, offering a quantitative knob for achieving controllable and predictable syntheses of noble-metal nanocrystals.[25,33] Typically, the reduction kinetics of a colloidal synthesis of metal nanocrystals can be described using the Finke−Watzky model,[34,35] with the involvement of two pseudoelementary steps:

$$A \rightarrow B \quad (1)$$

$$A + B^* \rightarrow 2B \quad (2)$$

where A, B, and B* represent the precursor molecule, metal atom, and active site on the seed, respectively. While the first reaction corresponds to the relatively slow reduction of the precursor in solution, the second step involves fast reduction on the surface of preexisting seeds, referred to as solution and surface reduction, respectively.[36] The rate of the first step pivotally affects the internal structures of the seeds generated during the nucleation stage, while the second step prevails in the following growth step. Because of the collision and electron transfer between the precursor and reductant, the reduction of

https://dx.doi.org/10.1021/acs.inorgchem.0c03576
Inorg. Chem. 2021, 60, 4182−4197

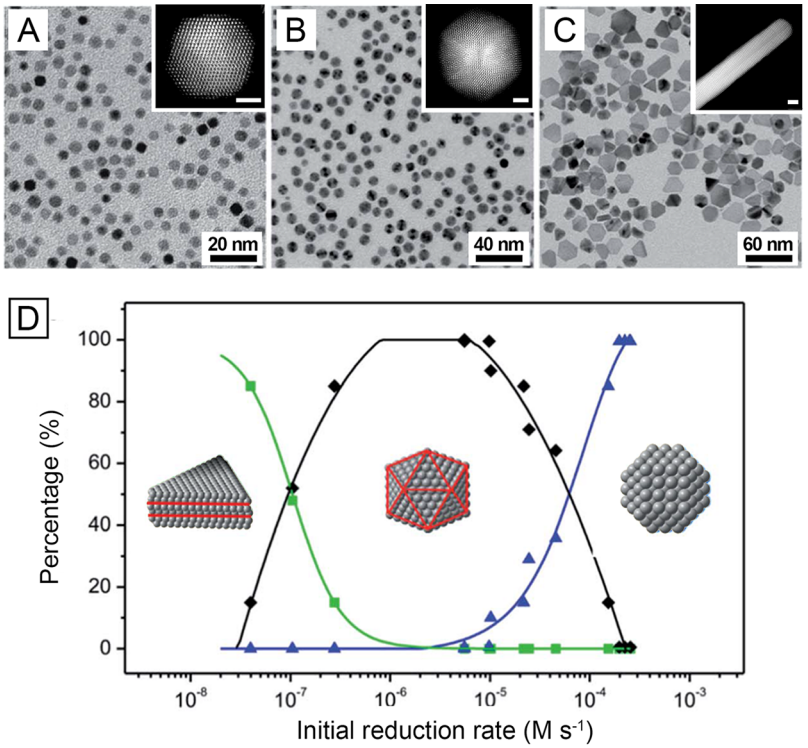

Figure 2. Importance of the initial reduction rate in controlling the internal structures of the seeds. (A–C) Transmission electron microscopy (TEM) images of Pd nanocrystals with different internal structures: (A) single-crystal, (B) multiply twinned, and (C) stacking-fault-lined, which were generated by varying the initial reduction rate of a polyol synthesis. The insets show the high-angle annular dark-field scanning TEM images of the individual nanocrystals in each sample, revealing their different internal twin structures. The scale bars in the insets are 2 nm. (D) Plot displaying the relative structure of Pd nanocrystals as a function of the initial reduction rate, showing the formation of single-crystal cuboctahedra (blue curve), multiply twinned icosahedra (black curve), and plates with stacking faults (green curve). Reproduced with permission from ref 37. Copyright 2015 American Chemical Society.

the precursor is expected to follow a second-order rate law, which is directly proportional to the concentrations of both reagents. However, because an excess amount of reducing agent is used in most syntheses, the rate law can be simplified into a pseudo-first-order reaction.[37,38] With techniques such as inductively coupled plasma mass spectrometry or ultraviolet–visible (UV–vis) spectroscopy, the concentration of the precursor can be tracked as a function of the reaction time, and the data are then fitted using the Finke–Watzky model. As such, the kinetic parameters of the reduction, including both the rate constant and activation energy, can be derived, generating quantitative data to correlate the reduction kinetics with the internal structures or shapes of the products. Once established, one can choose the appropriate experimental parameters to modulate the reaction kinetics for the production of nanocrystals with desired shapes, and even sizes and size distributions as demonstrated recently,[39,40] in a more or less rational manner.

This Viewpoint presents an overview of how reduction kinetics can be used to achieve a deterministic and predictable synthesis of colloidal noble-metal nanocrystals with well-controlled shapes. We begin with a discussion on the importance of the initial reduction rate in dictating the internal structures of the seeds, followed by an introduction to the kinetic control over both nucleation and growth of nanocrystals through manipulation of the reduction pathways. Case studies on Pd-based mono- and bimetallic systems are employed to demonstrate the significance of these mechanistic insights in controlling and even predicting the shape of the resultant nanocrystals. The speciation of the precursor affected by ligand exchange and coordination/dissociation of ligands is also highlighted, revealing how the introduction of additional ligands may alter the reduction rate of a precursor. In the end, we offer a summary of the current achievements and challenges, as well as our perspectives on the prospect of extending these methodologies to other noble metals.

2. CORRELATING THE INTERNAL STRUCTURE TO THE INITIAL REDUCTION RATE

In a colloidal synthesis of noble-metal nanocrystals, the shape taken by the final products has a strong correlation with the internal structures of the seeds formed at the very beginning.[33] Depending on the type and number of defects included, the seeds could take a single-crystal, singly twinned, multiply twinned, or stacking-fault-lined structure and subsequently grow into nanocrystals with distinct shapes under the direction of appropriate capping agents.[28] For single-crystal seeds, they can grow into cubes, octahedra, and rhombic dodecahedra, among others, whereas singly twinned seeds tend to evolve into bipyramids.[7,11] On the other hand, those seeds featuring multiple twin defects and stacking faults usually grow into multiply twinned particles (e.g., decahedra, icosahedra, and pentatwinned rods/wires) and plates, respectively. In a sense, any attempt to control the outcome of a synthesis must be built upon the ability to precisely maneuver the internal structures of the seeds. Both thermodynamics and kinetics play vital roles in directing the formation of a specific type of seed.[23,26] In a system controlled by thermodynamics, the most

https://dx.doi.org/10.1021/acs.inorgchem.0c03576
Inorg. Chem. 2021, 60, 4182–4197

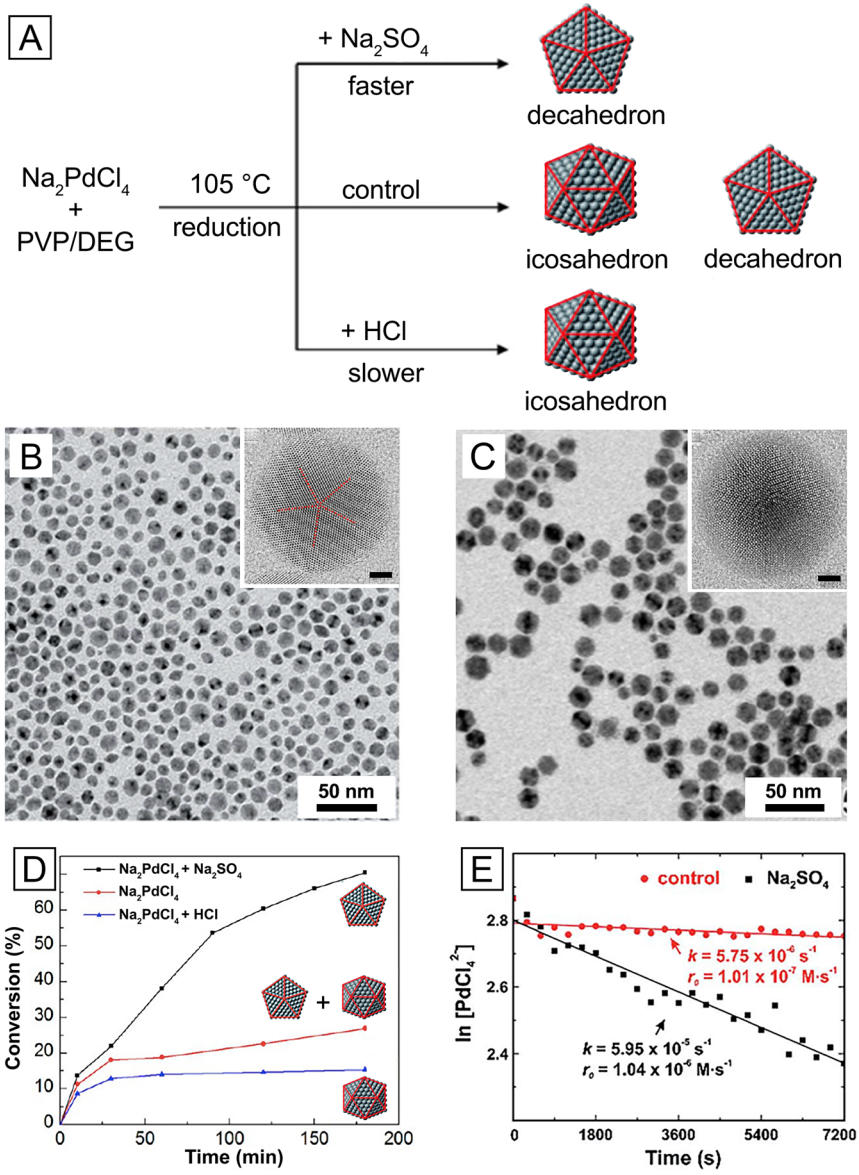

Figure 3. (A) Schematic illustration showing the maneuvering of reaction kinetics with additives to generate Pd decahedra and icosahedra in high purity. (B and C) TEM images of the decahedra and icosahedra, respectively. The insets show the corresponding high-resolution TEM images of an individual nanocrystal, with a scale bar of 2 nm. (D) Plot of the percent conversion of the Pd(II) precursor into Pd atoms as a function of the reaction time in the presence of different additives. (E) Plot of ln $[PdCl_4^{2-}]$ as a function of the reaction time for synthesis in the presence/absence of SO_4^{2-}, together with the corresponding rate constants (k) and initial reduction rates (r_0) labeled on the fitting curves. In the presence of an excess amount of reductant, the reduction of $PdCl_4^{2-}$ could be regarded as a pseudo-first-order reaction, and the data were fitted with first-order kinetics. (A–D) Reproduced with permission from ref 43. Copyright 2014 American Chemical Society. (E) Reproduced with permission from ref 42. Copyright 2016 American Chemical Society.

favorable structure is defined by a global minimum in the Gibbs free energy, where all energetic contributions (e.g., surface, volume, defects, and strain) are collectively minimized.[27] By the construction of a phase diagram as a function of the particle size and temperature, it was established that single-crystal seeds are favored at relatively large sizes, while multiply twinned seeds are more stable at a small length scale considering the increase in the strain energy with size.[41] Even though thermodynamics provides useful information on the most favored internal structure taken by the seeds at a given size, the experimental results often deviate from the theoretical predictions.[25] Under certain conditions with a significant barrier to surface diffusion, some seeds would rather settle into a local minimum in terms of free energy instead of reaching a global minimum, generating a thermodynamically less stable but kinetically favored product.[23] In this regard, maneuvering the internal structure taken by the seeds from a kinetic perspective would be a more viable strategy.

The initial reduction rate of a synthesis has been found to be crucial in determining the internal structures of the seeds, offering a quantitative knob for controlling the shape of the final products.[37] In a colloidal synthesis of metal nanocrystals, the reaction rate is expected to depend on the concentrations of both the reductant and metal precursor. In fact, for most of the synthetic protocols, the amount of reductant is in great excess, and thus the reduction of the precursor can be approximated to a pseudo-first-order reaction following the rate law: reaction rate (r) = k[A] = −d[A]/dt, where [A] is the

https://dx.doi.org/10.1021/acs.inorgchem.0c03576
Inorg. Chem. 2021, 60, 4182−4197

concentration of the metal precursor.[37,42] To obtain a specific type of seed, the initial reduction rate (r_0, r at $t = 0$), which is the reduction rate of the metal precursor in the nucleation stage of a synthesis, can be adjusted by varying a number of experimental parameters, including the reaction temperature, the type and concentration of the precursor, and the reducing power of the reductant. In a recent study involving the polyol synthesis of Pd nanocrystals, it was demonstrated that Pd truncated octahedra, icosahedra, and plates could be generated by adjusting the initial reduction rate through leverage of the different types of polyols and reaction temperatures (Figure 2A–C).[37] Specifically, when $PdCl_4^{2-}$ was reduced by ethylene glycol (EG) at 140 °C, the high initial reduction rate ($r_0 \approx 10^{-4}$ M s^{-1}) resulting from the strong reducing power of EG and high reaction temperature favored the formation of single-crystal seeds, generating truncated octahedra as the products. In contrast, the replacement of EG with diethylene glycol (DEG), which had a weaker reducing power, led to a moderate initial rate ($r_0 \approx 10^{-6}$ M s^{-1}) for the production of multiply twinned seeds and then icosahedra. Moreover, because of the substantially decelerated reduction rate ($r_0 \approx 10^{-8}$ M s^{-1}), plates with a stacking-fault-lined structure were obtained when $PdCl_4^{2-}$ was reduced by DEG at 75 °C. Taken together, seeds with single-crystal, multiply twinned, and stacking-fault-lined structures, respectively, were obtained as the initial reduction rate decreased (Figure 2D), generating nanocrystals with corresponding shapes as the final products. This quantitative correlation between the initial reduction rate and internal structures of the seeds offers a stronger capability of controlling the types of seeds generated in the initial stage, and thus the shapes of the nanocrystals evolved from them.

Manipulation of the reduction kinetics has also been successfully applied to synthesize multiply twinned nanocrystals in high purity, such as those having decahedral and icosahedral shapes, respectively.[42,43] Sharing similar features, Pd decahedra and icosahedra usually form simultaneously in the same batch of synthesis. Hence, fine-tuning the reduction rate into a proper regime is necessary for the production of only one type of seed and thus nanocrystals in a single shape. In one study, it was demonstrated that additives, such as Na_2SO_4 and HCl, could be introduced into a polyol synthesis of Pd nanocrystals to fine-tune the reduction kinetics for the formation of decahedral and icosahedral seeds, respectively (Figure 3A).[43] Without any additives, the as-obtained products were a mixture of decahedra and icosahedra. In contrast, the addition of Na_2SO_4 could speed up reduction of the Pd(II) precursor by promoting the oxidization of DEG to aldehyde, which served as the actual reductant, leading to the formation of decahedral seeds (Figure 3B). On the other hand, when HCl was introduced into the synthesis, both the decrease in the pH and the shift of equilibrium to the reactant side by an excess amount of Cl^- ions could slow down the reduction, giving rise to icosahedral seeds (Figure 3C). A quantitative study of the reduction kinetics by UV–vis further validated the effects of the additives on the synthesis of Pd decahedral and icosahedral nanocrystals (Figure 3D). A faster reduction rate was involved in the generation of decahedral seeds, while a slower one was preferred by icosahedral seeds. In another study involving the sulfate-mediated synthesis of Pd decahedra, the initial reduction rates for the sulfate-mediated and sulfate-free reactions were quantitatively measured to be 1.04×10^{-6} and 1.01×10^{-7} M s^{-1}, respectively (Figure 3E), further attesting to the role of Na_2SO_4 in accelerating reduction of the Pd(II) precursor and promoting the formation of decahedral seeds.[42]

In addition to decahedra, the formation of pentatwinned seeds is also a prerequisite for the generation of pentagonal rods/wires taking one-dimensional morphology.[44] As mentioned above, seeds with twin defects tend to be formed at a relatively slow reduction rate, which can be achieved by using a less-reactive precursor, a milder reducing agent, and/or a lower temperature.[37] Besides employing Pd decahedra as seeds for seed-mediated growth,[45] Pd pentatwinned rods and wires could also be obtained from a well-modified, one-pot synthesis, in which the Pd(II) precursor was reduced by DEG and ascorbic acid (AA) in the presence of NaI and HCl.[46] Particularly, the I^- and H^+ ions played vital roles in slowing down the reduction rate by coordinating with the precursor to form a PdI_4^{2-} complex and prohibiting the dissociation of AA to a stronger reductant, respectively. With the capping effect of I^- toward Pd{100} facets, the decahedral seeds then grew axially into pentagonal rods and then wires. According to quantitative analysis of the reduction kinetics, the initial reduction rate of the Pd(II) precursor was calculated to be 4.47×10^{-7} M s^{-1} for the I^--mediated reaction, and it became 1.62×10^{-5} M s^{-1} when I^- was replaced with Br^-. This result confirms the significant deceleration of reduction kinetics in the presence of I^-. With an increase in the concentration of the Pd(II) precursor or a decrease in the amount of NaI, impurities such as cubes and bipyramids appeared, confirming the importance of slow reduction kinetics in generating decahedral seeds and thus pentatwinned nanostructures.

Further slowing down the reduction rate will lead to the formation of plates, which are not thermodynamically favored products because of their large specific surface area and the presence of defects.[47] This structure is typically evolved from a seed lined with stacking faults. In a recent study on the preparation of Pd plates, hydroxylamine was judiciously selected as a reducing agent considering its mild reducing power to enable a slow reduction of the Pd(II) precursor for the generation of stacking-fault-lined seeds.[48] With citric acid serving as the capping agent toward Pd{111} facets, the seeds eventually grew into plates with a well-defined hexagonal shape and multiple planar defects lying parallel to the basal planes. Through UV–vis measurements, the concentration of the remaining precursor was tracked over time, and the initial reduction rate was determined to be 3.6×10^{-7} M s^{-1}, which fell into the previously reported rate range required for the formation of stacking-fault-lined seeds.

Taken together, precise control over the reduction kinetics is crucial in obtaining seeds with the desired internal structures and thus nanocrystals with well-controlled shapes in high purity. Specifically, as the initial reduction rate decreases, the seeds generated in the early stage will switch from single-crystal to multiply twinned and finally stacking-fault-lined structure.[37] Kinetic control over the reaction can leverage the employment of metal precursors and reductants with appropriate reactivity, introduction of additives to alter the precursor structure, regulation of the reducing power of reductants, and use of an appropriate reaction temperature.[43,49,50] More recent studies have also demonstrated that the aforementioned relationship between the reduction kinetics and the internal structures of the seeds can also be extended to other noble-metal nanocrystals.[51] Although the exact values of the initial reduction rates for the formation of each type of seed may vary for different metal systems, it should be noted that they

https://dx.doi.org/10.1021/acs.inorgchem.0c03576
Inorg. Chem. 2021, 60, 4182–4197

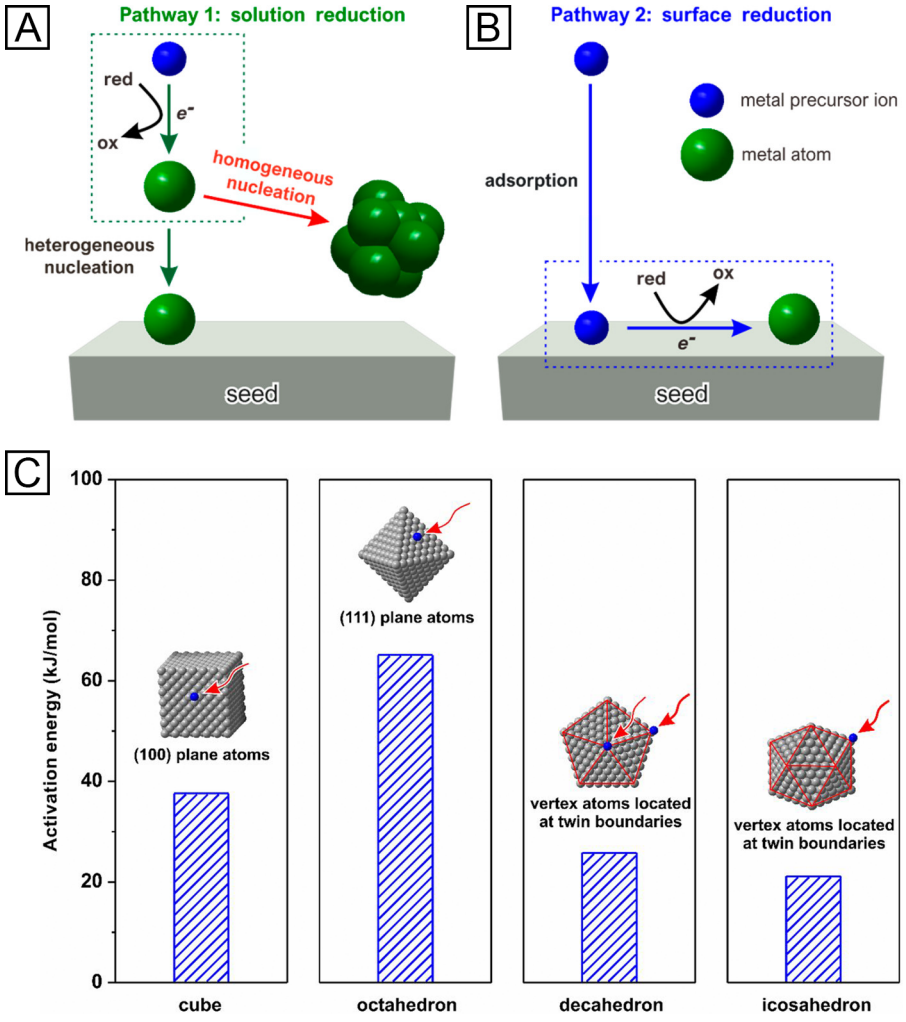

Figure 4. (A and B) Schematic illustrations showing two reduction pathways potentially taken by a precursor in the synthesis of metal nanocrystals: (A) solution reduction and (B) surface reduction, respectively. (C) Comparison of the activation energy (E_a) for autocatalytic surface reduction on Pd seeds with different facets and twin structures. The insets show the preferential sites for the nucleation and deposition of Pd atoms through autocatalytic surface reduction. (A and B) Reproduced with permission from ref 36. Copyright 2017 American Chemical Society. (C) Reproduced with permission from ref 55. Copyright 2017 National Academy of Sciences, USA.

generally should follow the same trend as that stated above for Pd. The ability to produce a specific type of seed through manipulation of the reduction kinetics offers a reliable approach to the deterministic and predictable synthesis of noble-metal nanocrystals with the desired properties.

3. CONTROLLING BOTH NUCLEATION AND GROWTH THROUGH A KINETIC APPROACH

In addition to controlling the internal structure of the seeds formed during nucleation, manipulating the subsequent growth pattern of the seeds is also critical in generating noble-metal nanocrystals with well-controlled shapes. To this end, a comprehensive understanding of the reduction of precursors in both the nucleation and growth stages is of great necessity. Typically, two different reduction pathways may be involved during these processes.[36] The metal ions can either be directly reduced to atoms in the solution or adsorb onto the surface of the already formed seeds, followed by their reduction to atoms. In a sense, solution and surface reduction, respectively, are engaged in these two pathways (Figure 4A,B). In a one-pot synthesis, solution reduction dominates in the initial stage because of the absence of a preexisting surface, and seeds have to be formed through homogeneous nucleation (or self-nucleation). It is worth pointing out that recent studies also demonstrated that dusts commonly present in the reaction could potentially affect the nucleation process and thus questioned the classical homogeneous nucleation theory, but the underlying mechanism and generality of this phenomena is yet to be elucidated.[52−54] Once there are seeds (generated in situ or introduced into the system), both reduction pathways can be taken by the precursor for the following growth of seeds into nanocrystals. On the basis of quantitative analysis of the reduction pathways taken by different Pd(II) precursors, slow reduction kinetics was found favoring surface reduction, while solution reduction is more likely to be adopted under fast reduction rates.[36] By finely tuning the experimental parameters such as the type of precursor and reaction temperature, one can switch between different reduction pathways to generate nanocrystals with the desired shapes and properties.

Under the proper kinetic conditions, reduction of the precursor can preferentially take place on the surface of seeds for growth because of the lower activation energy barrier and associated autocatalytic process. The heterogeneity in the

https://dx.doi.org/10.1021/acs.inorgchem.0c03576
Inorg. Chem. 2021, 60, 4182−4197

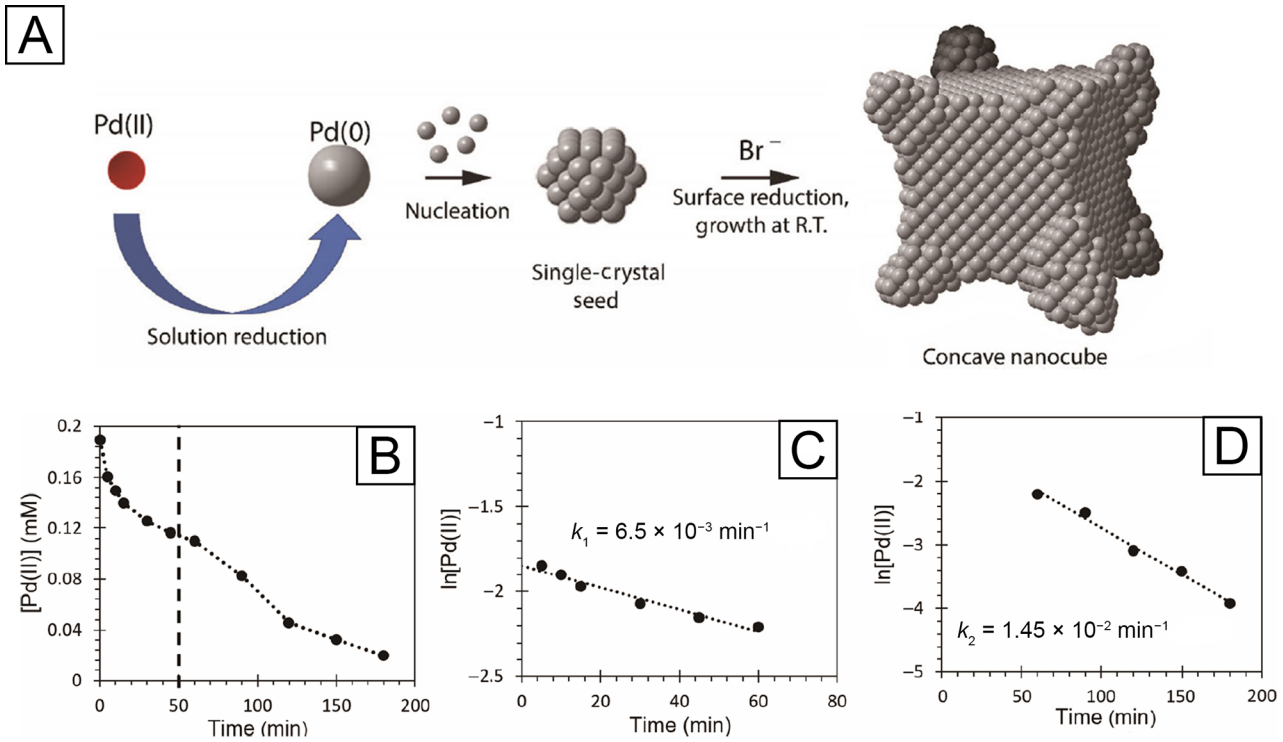

Figure 5. (A) Schematic illustration showing the formation of Pd concave cubes with a one-pot, two-step method. (B) Plot of the concentration of Pd(II) ions remaining in the reaction solution over time. The dashed line indicates the separation of two different trends. (C and D) First-order kinetic plot of ln [Pd(II)] over time showing a linear function for the trends (C) from 0 to 60 min and (D) from 60 to 180 min of the reaction, respectively. The corresponding rate constants (k) are labeled on the fitting curves. Adapted with permission from ref 58. Copyright 2018 Springer Nature.

surface structure, including different types of facets and the presence/absence of twin boundaries on the seeds, thus has a profound impact on the growth pattern.[55] On the basis of the Finke–Watzky model and Arrhenius plot, the activation energies of surface reduction for a precursor on different facets can be derived and compared. Taking Pd nanocrystals as an example, the energy barrier for reduction of the Pd(II) precursor on a capping-free cubic seed is around half that on an octahedral seed, suggesting the easier growth of atoms on {100} facets relative to {111} (Figure 4C). This could be ascribed to the higher surface energy of {100} relative to {111} facets in the absence of capping agents, making them more preferred for the deposition of atoms.[23] Further study of the autocatalytic surface reduction on cubic seeds with different sizes suggested preferential growth on {100} facets instead of edges and corners.[55] Although smaller cubes possess a larger proportion of surface atoms, especially more undercoordinated atoms on edges and corners, which might lower the energy barrier for growth,[13,56,57] the difference in the activation energies resulting from the size effect is actually very small. As such, autocatalytic surface reduction exhibited negligible dependence on the sizes of seeds. In addition to the facet type, the presence of twin boundaries also plays a pivotal role. For multiply twinned seeds, their vertex sites intersected by multiple twin boundaries often exhibit lower activation energy barriers than the side faces, making them a prior choice for the autocatalytic surface reduction. Both the low-coordinated atoms and significant surface strain, which may further alter the electronic structure of surface atoms, contribute to the reduction preference at vertices. With Pd decahedra and icosahedra serving as seeds, concave structures with spikes protruding from the vertices were obtained when additional Pd(II) precursor was introduced, confirming the faster growth of Pd on the vertex sites.[55]

With a deeper understanding of the reduction pathways taken by metal precursors, the synthesis of nanocrystals can now be more rationally pursued. In particular, when a proper precursor and reductant are chosen, it is feasible to control the nucleation and growth separately to obtain the desirable seeds and direct their growth, moving toward a predictable synthesis of nanocrystals. A good example can be found in Pd concave cubes synthesized through a one-pot method (Figure 5A).[58] Kinetic analysis revealed the involvement of a two-step reaction, with nucleation and growth of the Pd nanocrystals temporally separated and each being dominated by a distinctive reduction pathway (Figure 5B). The employment of sodium ascorbate as a strong reductant enabled the initial formation of single-crystal seeds in the solution phase (Figure 5C).[38] As the reaction proceeded, the decrease in the precursor and reductant concentrations coupled with an increase in the number of seeds led to a switch to surface reduction in the growth step (Figure 5D). The greater rate constant in the growth step (1.45×10^{-2} min^{-1}) relative to that in the nucleation step (6.5×10^{-3} min^{-1}) also confirmed the lower energy barrier associated with surface reduction compared to that of solution reduction. In the presence of Br^- ions and a relatively low reaction temperature, the Pd{100} facets were selectively blocked, and the diffusion of atoms was significantly slowed down. As a result, the newly formed Pd atoms piled up at the corners/edges of the seeds where the surface energy is higher than that at other sites, giving rise to a concave structure for the products. The key to this synthesis is

https://dx.doi.org/10.1021/acs.inorgchem.0c03576
Inorg. Chem. 2021, 60, 4182–4197

the combination of a strong reductant with a low reaction temperature. The former enabled a fast initial reduction rate of the precursor to generate single-crystal seeds, while the latter guaranteed the dominance of surface reduction in the growth stage and the suppression of atom diffusion to promote the site-selected growth. The high-index facets, together with the large specific surface area, give promise to the Pd concave nanocubes as active catalysts for various reactions.

A similar example was demonstrated in the synthesis of Pd arrow-headed tripods.[59] The slow initial reduction rate led to the generation of triangular, platelike seeds, and they further catalyzed the dehydrogenation of benzyl alcohol, the solvent, to benzaldehyde and H atom. The as-formed H atoms dramatically accelerated reduction of the Pd(II) precursor, facilitating the overgrowth of Pd atoms at the tips of the seeds and thus the evolution of seeds into tripods with a concave structure. Encouraged by these results, we can expect the production of more complex structures using a one-pot method through careful control of the reduction kinetics. The enrichment in nanocrystals with novel shapes and superior properties may greatly benefit their applications in a myriad of fields.

In the synthesis involving only a single reducing agent, once it is mostly consumed, the reduction rate will experience a sharp decrease and become hard to control. As an improvement, the reduction kinetics can be better manipulated by intentionally introducing dual reductants with different reducing powers. One example is the production of Pd octahedra in a one-pot setting.[60] The synthesis could be distinctively separated into two steps: (i) a strong reductant (e.g., AA or hydroquinone) was used to generate single-crystal seeds in the initial stage of the synthesis, and (ii) upon depletion of the strong reductant, a weak reducing agent (e.g., citric acid) would take over to slowly reduce the unreacted precursor and stabilize the {111} facets for the generation of octahedral nanocrystals. In this case, solution reduction was adopted in the beginning, and its dominance was switched to surface reduction once seeds were formed. The weak reducing power of citric acid and the resultant slow reduction rate also ensured the dominance of surface reduction in the growth step, suppressing self-nucleation and thus generation of the undesired small Pd particles. Compared to the case of a single reductant, the introduction of a second reducing agent not only enables a more complete conversion of the precursor but also makes the growth of nanocrystals more controllable. For example, if a relatively strong reducing agent is used at the growth stage, the faster atom deposition rate may lead to the formation of concave structures instead of plain nanocrystals. Combined with different capping agents, nanocrystals enclosed by various types of facets can also be obtained. Aside from dual reductants, effective control of the reduction kinetics may be achieved through leverage of the dual precursors in an individual synthesis.[61] Such a strategy is also extendible to metals other than Pd, enriching and simplifying the synthesis of metal nanocrystals with diverse shapes and properties.

In addition to the one-pot method with well-separated nucleation and growth steps, depositing atoms onto preformed seeds is also widely used for the shape-controlled synthesis of nanocrystals. Variation in the reduction kinetics may lead to different growth patterns, resulting in the formation of nanocrystals with varying shapes. For example, using a similar protocol, both Pd octahedra and tetrahedra could be generated from cuboctahedral seeds by simply switching the precursor from Na_2PdCl_4 to $Pd(acac)_2$.[62] The relatively weak binding of $[acac]^-$ ligands to Pd(II) ions led to a faster reduction rate of $Pd(acac)_2$ and thus a quick drop in its concentration [only 22.9% of the Pd(II) precursor remained in the solution at 0.5 min into the reaction]. As a consequence, after the cuboctahedral seed evolved into an octahedral shape, the remaining precursor was only available for the growth of Pd atoms on four of the eight {111} facets of the octahedron, generating tetrahedral products with reduced symmetry relative to the seeds. In contrast, the reduction rate was greatly slowed down when Pd(II) ions were coordinated by Cl^- [79.1% of the Pd(II) precursor was unreacted at 0.5 min]. The high abundance of precursor around the seed enabled the nucleation of atoms on all eight {111} facets of the cuboctahedral seeds and thus the formation of Pd nanocrystals with an octahedral shape for preservation of the symmetry. A similar example can be found in the epitaxial growth of Ag or Au on Pd nanocubes.[63] Through control of the reduction kinetics, Ag or Au can be selectively deposited onto a certain number of side faces (ranging from one to six) of a cubic Pd seed, giving rise to the formation of bimetallic nanocrystals with varied asymmetric/symmetric shapes. Such site-selected growth may inspire the synthesis of nanocrystals with more complex structures and potentially novel properties.

4. EXTENSION FROM A MONOMETALLIC TO A BIMETALLIC SYSTEM

In addition to the monometallic system, bimetallic nanocrystals with distinctive shapes, structures, and elemental distributions can be synthesized through a one-pot method by fine control of the reduction kinetics.[64−67] When two precursors are involved, a significant difference in their reduction rates may lead to sequential reduction of the precursors and thus the formation of a core−shell structure, while similar reduction rates favor the production of alloy nanocrystals (Figure 6A). For example, when Na_2PdCl_4 and K_2PtCl_4 were simultaneously reduced by EG, the 10-times-greater initial reduction rate of the Pd(II) precursor relative to that of Pt(II) (2.50×10^{-4} and 2.49×10^{-5} M s^{-1} for $PdCl_4^{2-}$ and $PtCl_4^{2-}$, respectively) resulted in the fast generation of Pd seeds, followed by the slow reduction and deposition of Pt atoms onto them.[68] Consequently, $Pd@Pt_{1.9L}$ nanocrystals with a core−shell structure and a thermodynamically favored octahedral shape were obtained as the final product (Figure 6B). In contrast, if an additional amount of KBr was introduced, the stronger binding of Br^- to Pd(II) and Pt(II) ions led to the formation of $PdBr_4^{2-}$ and $PtBr_4^{2-}$ complexes, respectively.[69,70] The ligand exchange greatly decelerated the reduction of both precursors and narrowed the gap between their initial reduction rates (5.36×10^{-5} and 2.25×10^{-5} M s^{-1} for $PdBr_4^{2-}$ and $PtBr_4^{2-}$, respectively, in the presence of 63 mM KBr). As a result, the Pd and Pt atoms were generated and incorporated into nanocrystals at comparable rates, giving rise to Pd−Pt alloy nanocrystals as the products. The presence of Br^- ions also contributed to the formation of a cubic shape for the alloy nanocrystals because of their selective capping toward both Pd{100} and Pt{100} facets (Figure 6C).

Using a similar protocol in the absence of KBr but switching K_2PtCl_4 to $Pt(acac)_2$, reduction of the Pt(II) precursor could be further slowed down with the ratio of the initial reduction rates of the Pd(II) and Pt(II) precursors enlarged to around 100 times (2.34×10^{-4} and 2.40×10^{-6} M s^{-1}, respectively).[71] The extremely slow reduction of the Pt(II) precursor and the

https://dx.doi.org/10.1021/acs.inorgchem.0c03576
Inorg. Chem. 2021, 60, 4182−4197

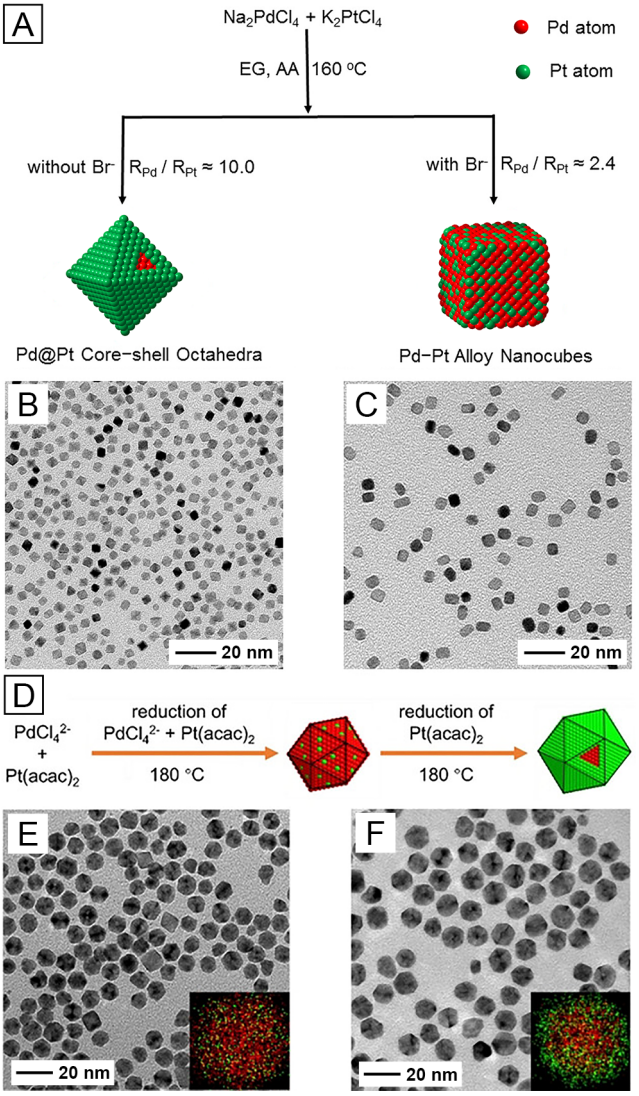

Figure 6. (A) Schematic illustration showing manipulation of the reduction kinetics to generate Pd–Pt bimetallic nanocrystals with different shapes and elemental distributions. (B and C) TEM images of (B) Pd@Pt core–shell octahedra and (C) Pd–Pt alloy cubes, respectively. (D) Schematic illustration showing the sequential generation of Pd–Pt alloy icosahedral seeds and deposition of a Pt shell in the formation of Pd@Pt core–shell icosahedral nanocrystals using a one-pot approach. (E) TEM image of the Pd–Pt alloy icosahedra obtained at 1 min into the synthesis. (F) TEM image of the Pd@Pt core–shell icosahedra obtained at 3 h into the synthesis. The insets show the energy-dispersive X-ray mapping of individual nanocrystals, indicating the different elemental distributions. The red and green colors represent Pd and Pt, respectively. (A–C) Adapted with permission from ref 68. Copyright 2016 American Chemical Society. (D–F) Reproduced with permission from ref 72. Copyright 2019 Wiley-VCH.

high reaction temperature enabled the relatively fast diffusion of Pt atoms to cover the entire surface of Pd seeds, contributing to the formation of Pd@Pt core–shell octahedra with a Pt shell thickness of only one atomic layer. The ultrathin Pt shell terminated in {111} facets not only guaranteed a high catalytic activity toward the oxygen reduction reaction but also minimized the quantity of Pt and the cost of the catalyst. When such a strategy is applied to metals with high prices, catalysts with improved performance, higher cost efficiency, and a simplified synthetic method can be achieved.

Moreover, when EG is replaced with tetraethylene glycol (TTEG) as a milder reducing agent, the reduction of both precursors could be further decelerated, leading to the formation of multiply twinned, icosahedral nanocrystals.[72] Similar to previous cases, because of the large difference between the initial reduction rates of Na_2PdCl_4 and $Pt(acac)_2$ (2.8×10^{-5} and 1.8×10^{-7} M s^{-1}, respectively), the two precursors were sequentially reduced, generating products with a core–shell structure (Figure 6D–F). Different from Pd@Pt octahedra, the slower reduction of the Pd(II) precursor in TTEG favored the formation of multiply twinned seeds, which finally evolved into an icosahedral shape. The thin thickness of the Pt shell, enclosure of {111} facets, and presence of twin boundaries all contributed to the high mass and specific activities of the Pd@Pt icosahedra. When subjected to an etching solution containing $FeCl_3$, KBr, and HCl, the Pd core could be selectively removed, generating Pt nanocages with further enhanced catalytic performance. By taking advantage of the reduction kinetic gap between different metal precursors, not only alloy but also core–shell nanocrystals with various shapes, structures, and compositions are expected to be synthesized using a one-pot setting, without the involvement of seed-mediated growth. Considering the simplicity of the protocol, such a one-pot synthesis can also be integrated with continuous-flow reactors,[71] scaling up the production of nanocrystals with well-controlled quality and catalytic performance.

5. SPECIATION OF THE PRECURSOR AND ITS IMPACT ON THE REDUCTION KINETICS

Because of the close correlation between the reduction kinetics of a synthesis and the resultant nanocrystals, it is pivotal to pose tight control over reduction of the precursors. The reduction rate can be affected by a number of experimental parameters, such as the reaction temperature, the type of precursor and reductant, and their concentrations. Of particular importance, a vital factor that could substantially alter the reduction rate is speciation of the precursor actually involved in the synthesis. Because of the coordination effect from the solvents or other ligands introduced into the synthesis, the original ligand to the metal ion in the precursor could be partially or completely replaced, generating new complexes different from the original one and thus affecting the reduction kinetics and pathways. To this end, a number of studies have paid close attention to the speciation of the precursor in a synthesis and its impact on the outcome of the synthesis. A number of techniques, including UV–vis spectroscopy,[35,73−76] mass spectroscopy,[35,76,77] X-ray absorption spectroscopy,[76,77] and nuclear magnetic resonance (NMR) spectroscopy,[77] have been applied to shed light on the speciation.

For the synthesis of Pd nanocrystals, $PdCl_4^{2-}$ and $PdBr_4^{2-}$ are two commonly used precursors, with the latter featuring a slower reduction rate because of its more negative reduction potential ($PdCl_4^{2-}$/Pd = 0.62 V and $PdBr_4^{2-}$/Pd = 0.49 V vs reversible hydrogen electrode).[78,79] Besides, it has also been reported that $PdBr_4^{2-}$ prefers to take a surface reduction pathway in the presence of preformed seeds because of the lower energy barrier associated with this pathway.[36] However, it is often overlooked that when dissolved in water, the precursors could be hydrated, with partial ligands replaced by

https://dx.doi.org/10.1021/acs.inorgchem.0c03576
Inorg. Chem. 2021, 60, 4182−4197

water molecules, existing in the form of $[PdX_n(H_2O)_{4-n}]^{2-n}$ (X = Cl^- or Br^-, n = 0–4).[73,80,81] Speciation of the Pd(II) complexes can be differentiated by UV–vis spectroscopy through their absorption peaks,[81] and their reduction rates vary drastically as the halide ions are substituted by water in the complexes.[73,80]

In particular, the introduction of additional halide ions into the solution can essentially suppress hydrolysis of the Pd(II) precursor and exchange ligands with it, altering the dominant precursor species present in the reaction. A recent study quantitatively analyzed the influence of halide ions on the speciation of the Pd(II) precursor and thus the growth pattern of Pd nanocrystals.[73] In a comparison of the UV–vis spectra recorded from aqueous solutions of Pd(II) precursors with/without the addition of halides (Na_2PdCl_4, K_2PdBr_4, Na_2PdCl_4 plus KCl, and Na_2PdCl_4 plus KBr), the shift of the peak positions clearly indicated the change in the speciation of the precursor (Figure 7A). Specifically, the Pd(II) precursors in pure water were partially hydrated to generate a mixture of $PdX_2(H_2O)_2$ and $PdX_3(H_2O)^-$ (X = Cl^- or Br^-), while the

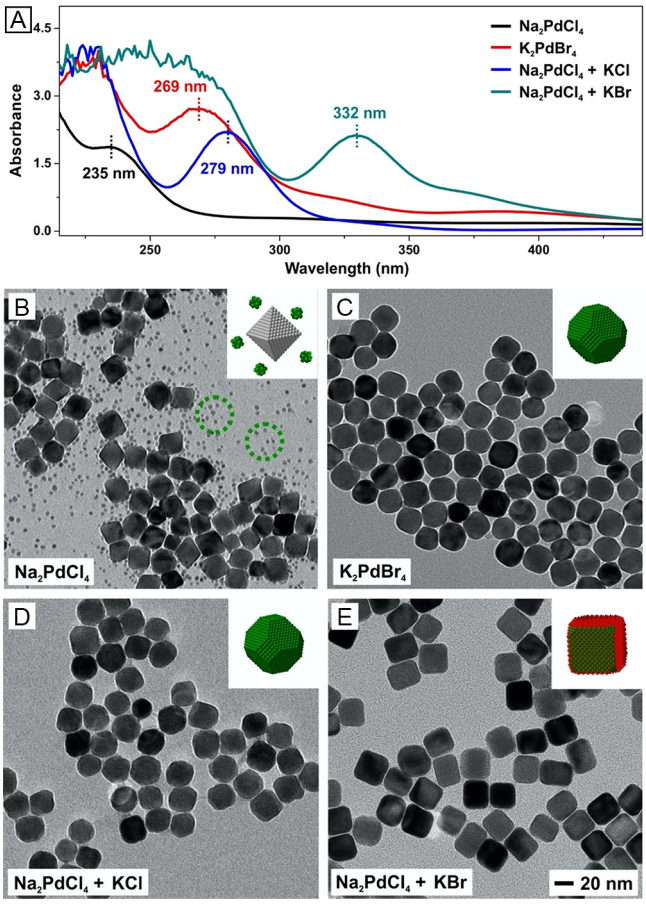

Figure 7. (A) UV–vis spectra recorded from aqueous solutions of Pd(II) precursors in the absence/presence of halides, indicating the generation of Pd(II) species in different forms. (B–E) TEM images of the products obtained from Pd octahedral seeds using aqueous solutions of (B) Na_2PdCl_4, (C) K_2PdBr_4, (D) Na_2PdCl_4 plus KCl, and (E) Na_2PdCl_4 plus KBr as the precursors to Pd, respectively. The insets show the atomic models of the corresponding products, with the gray, green, and red dots denoting the existing Pd atoms, newly formed Pd atoms, and Br^- ions, respectively. The scale bar in panel E applies to all other panels. Reproduced with permission from ref 73. Copyright 2020 Wiley-VCH.

major species was maintained as PdX_4^{2-} in the presence of excess halide ions. Moreover, the addition of KBr to a Na_2PdCl_4 solution could convert $PdCl_4^{2-}$ to $PdBr_4^{2-}$ through a ligand-exchange process, as suggested by the absorption peak at 332 nm corresponding to $PdBr_4^{2-}$. When used as precursors in the seed-mediated growth of Pd octahedral nanocrystals, the four types of Pd(II) species gave rise to different products, owing to variation in the reduction kinetics and reduction pathways. As shown in Figure 7B–E, the generation of additional small particles instead of the growth of seeds was observed in the case of Na_2PdCl_4, while the octahedral seeds grew into truncated octahedra and then cubes when K_2PdBr_4/Na_2PdCl_4 plus KCl and Na_2PdCl_4 plus KBr were used, respectively. By quantitative measurement of the reduction kinetics, it was found that the reduction rates of the different Pd(II) precursors decreased in the order of Na_2PdCl_4 > K_2PdBr_4 > Na_2PdCl_4 plus KCl > Na_2PdCl_4 plus KBr, which could be ascribed to a decrease in the reduction potential of the precursor actually active in the reaction [$PdX_2(H_2O)_2$ and $PdX_3(H_2O)^-$ > $PdCl_4^{2-}$ > $PdBr_4^{2-}$].[80] Moreover, in the presence of preformed seeds, different speciations of the precursor also led to alteration in the reduction pathway, with aqueous Na_2PdCl_4 preferring solution reduction and the others favoring surface reduction. As such, the use of aqueous Na_2PdCl_4 as a precursor resulted in a fast reduction rate and the formation of small particles via homogeneous nucleation in the solution phase. In contrast, the reduction rate was substantially decelerated, and reduction of the precursor on the surface of seeds was favored in the other three cases, leading to the growth of seeds into larger nanocrystals. In particular, with excess Br^- ions serving as a capping agent toward Pd{100} facets, well-defined cubes were obtained as the final product when Na_2PdCl_4 plus KBr was employed as the precursor. Furthermore, by variation of the molar ratio of KBr to Na_2PdCl_4, the percentage of Pd(II) converting to $PdBr_4^{2-}$ would change correspondingly. Thus, the reduction rate could be tuned, and the reduction pathway could be switched between surface and solution reduction, with a higher ratio favoring slower reduction kinetics and thus surface reduction. A similar trend was observed when Pd nanocubes were used as seeds for growth. In another study on the synthesis of Au@Pd concave nanocubes, it was also found that ligand exchange between the Pd(II) precursor and halide ions released from the capping agent played a significant role in controlling the morphology of resultant nanocrystals.[79] Taken together, the reduction kinetics, reduction pathways, and thus the outcome of a synthesis could essentially be affected by halide ions involved in the reaction due to variation in the speciation of the precursor through ligand exchange.

In addition to aqueous routes, organic solvents or other additives added to oil-phase syntheses of Pd nanocrystals can also act as ligands to coordinate with the Pd center in the precursor, altering the reduction kinetics. In one report, Pd nanocrystals with various shapes were obtained by reducing $Pd(acac)_2$ with formaldehyde in the presence of different amounts of oleylamine (OAm).[74] The UV–vis spectra of reaction solutions showed that different Pd(II) intermediates were formed in the form of $[Pd(acac)_x(OAm)_y]$ when the concentration of OAm was changed. Specifically, with more OAm introduced into the synthesis, a decrease in the reduction rate was experimentally observed as a result of replacement of the $[acac]^-$ ligand by OAm in the complex. Meanwhile, Pd icosahedra, a mixture of decahedra and tetrahedra, and a

https://dx.doi.org/10.1021/acs.inorgchem.0c03576
Inorg. Chem. 2021, 60, 4182–4197

mixture of octahedra and plates were sequentially obtained. However, this trend seems contradictory to the expectation that nanocrystals would switch from single-crystal to multiply twinned and finally stacking-fault-lined structures as the reduction rate decreased. It should be pointed out that OAm served as not only a ligand to the precursor but also a capping agent capable of altering the surface free energy of Pd nanocrystals. Consequently, the final shape taken by Pd nanocrystals is an outcome of the complicated interplay between thermodynamic and kinetic controls. Moreover, a recent study also demonstrated the critical roles of ligand binding with both the metal precursor and nanoparticle surface in controlling the rates of nucleation and growth and thus the size of the resultant nanoparticles.[82] Specifically, a kinetic descriptor, (growth-to-nucleation rate ratio)$^{1/3}$, was employed to predict the nanoparticle size despite different metals and synthetic conditions. Thus, although the introduction of ligands to a synthesis offers an additional knob for controlling the speciation of the precursor and thus the reduction kinetics, their interaction with the nanocrystal surface and the consequent influence on the shape and size of the product should also be noted cautiously.[28]

Moreover, efforts have also been devoted to identifying the actual precursor involved in the synthesis of other metal nanocrystals besides Pd and investigating its influence on the products. For example, quantitative analysis of an oil-phase synthesis of Pt nanocrystals, during which $Pt(acac)_2$ was reduced by CO in the presence of OAm and oleic acid (OA), revealed that ligand replacement and anion exchange had profound impacts on the growth of nanocrystals.[35] With excess OAm present in the reaction, the Pt nanocrystals evolved from quasi-spherical particles to cubes with larger sizes as the amount of OA was increased. An examination of the Pt complexes formed prior to the reaction revealed that $Pt(OAm)_4(acac)_2$ was generated in the absence of OA, which featured fast reduction kinetics due to the involvement of autocatalytic surface reduction. When the experimental data were fit with the Finke−Watzky model, the rate constant for solution reduction and the apparent rate constant obtained after the incorporation of other parameters for surface reduction were found to be k_1 = 0.0034 min^{-1} and k_2' = 0.96 min^{-1}, respectively. In contrast, when OA was introduced to the reaction at a molar ratio of 4:1 with $Pt(acac)_2$, a precursor in the form of $Pt(OAm)_4(OA)_2$ was generated and reduced at a much slower rate with autocatalytic reduction switched off likely because of the absence of enough seeds (k_1 = 0.0022 min^{-1} and k_2' = 0.002 min^{-1}). In another study, it was found that the reduction of H_2PtCl_6 by methanol was accelerated with the addition of water.[76] Specifically, the water molecules could coordinate with the precursor $[PtCl_5(CH_3O)]^{2-}$ and intermediate $[PtCl_3(CH_3O)]^{2-}$, generating $[PtCl_5(CH_3O)(H_2O)]^{2-}$ and $[PtCl_3(CH_3O)(H_2O)]^{2-}$ with much lower activation energy for reduction and thus resulting in faster reduction kinetics. Another intriguing example can be found in the synthesis of one-dimensional Ag nanocrystals, in which slowing down the reduction kinetics for anisotropic growth was achieved through the addition of a capping agent containing Cl^- ions.[83] The reaction between Cl^- and Ag(I) ions led to the generation of solid AgCl, which served as the actual precursor to elemental Ag. The impact of ligands on the speciation of the precursor and thus the reduction kinetics and resultant nanocrystals has also been reported for Cu.[61,77] Detailed calculations and understanding of the nucleation mechanism induced by ligand dissociation are also reported for Ir nanoparticles.[84,85] Owing to the significant influence of precursor−ligand interactions, more endeavors to identify the actual precursor in a synthesis are expected in the future for a deeper understanding and tighter control over the reduction kinetics of the colloidal synthesis of metal nanocrystals. Most importantly, in the future, all syntheses involving kinetic control should be accompanied by quantitative analysis of the kinetic parameters to enable the analysis and prediction over the shape, size, and size distribution of the resultant nanocrystals.[33,39,40]

Caution! *All of the chemicals used in the synthetic procedures cited in this work should be handled in accordance with safety practices. The organic solvents, such as EG and DEG, and other chemicals that are potentially hazardous should be treated with extra caution.*

6. CONCLUSIONS AND PERSPECTIVES

Unveiling the correlation between the reduction kinetics of a synthesis and the resultant nanocrystals is critical to the production of metal nanocrystals in a controllable and predictable manner. With Pd as an example, quantitative analysis reveals that the reduction rate in the nucleation stage plays a deterministic role in the generation of seeds taking different internal structures. Specifically, as the reduction rate decreases, the seeds generated during the nucleation stage will switch from single-crystal to multiply twinned and finally stacking-fault-lined structures, which further develop into nanocrystals with different shapes in the following growth stage. With insights into the impact of reduction kinetics on a synthesis, it is feasible to manipulate the reduction rates and pathways during nucleation and growth separately to obtain desirable seeds and regulate the growth patterns of nanocrystals, thereby posing tighter control over the products. Moreover, the methodology can be extended to the bimetallic system with dual precursors present in the solution, enabling the one-pot synthesis of nanocrystals taking a core−shell or alloy structure by judiciously manipulating the reduction sequence of the precursors. Importantly, extra precautions should be taken for speciation of the precursor actually involved in a synthesis, which can be altered by ligands, solvents, or other additives through coordination and ligand exchange, resulting in changes to the reduction kinetics. With a focus on Pd nanocrystals, we have demonstrated that manipulation of the reduction kinetics offers a reliable knob for the well-controlled synthesis of metal nanocrystals. It should be noted that, although a high electron dose may induce potential shape and even structural change in nanocrystals during TEM imaging, controlling the electron dose rate and shortening the exposure time have become common practices to minimize the beam effect,[86] suggesting the reliability of TEM analysis discussed in this Viewpoint. Besides, the oxidation of noble-metal nanocrystals, such as Pd and Pt, by the oxygen from air is relatively slow, and surface oxides are hardly resolved in the final products using either X-ray photoelectron spectroscopy or high-resolution TEM, indicating the negligible influence from surface oxidation on the shape or structure of nanocrystals.[87] The presence of capping agents on the surface of a nanocrystal would also significantly decelerate the oxidation process.

In addition to the success in correlating the reduction kinetics with the internal structures and shapes of Pd nanocrystals, it is anticipated that the methodology is

https://dx.doi.org/10.1021/acs.inorgchem.0c03576
Inorg. Chem. 2021, 60, 4182−4197

extendible to the colloidal synthesis of nanocrystals made of other noble metals. In a recent study on the synthesis of Pt nanocrystals by reducing a Pt(IV) precursor with glucose, it was demonstrated that Pt octahedra and concave cubes could be obtained at a low and high concentration of glucose, respectively (Figure 8A–C).[88] Quantitative analysis of the

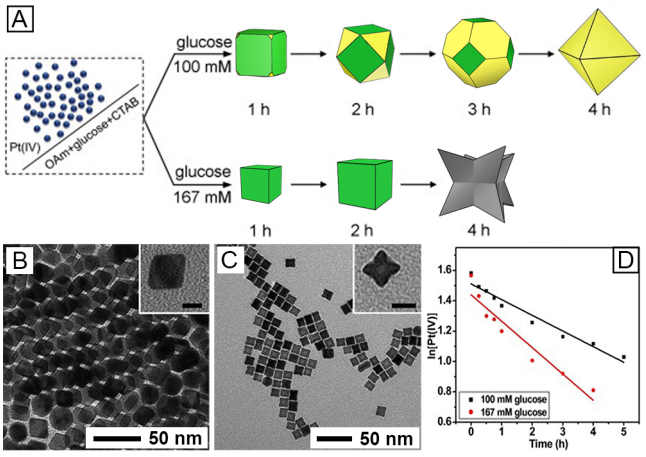

Figure 8. (A) Schematic illustration showing the synthesis of Pt octahedra and concave cubes using the same protocol but different concentrations for the reductant. (B and C) TEM images of the as-obtained (B) octahedra and (C) concave cubes, respectively, with the insets showing the individual nanocrystals at a higher magnification. The scale bars in the insets are 10 nm. (D) Plots showing the pseudo-first-order reduction kinetics involving the use of glucose at different concentrations, demonstrating the correlation between the reduction kinetics and shape of the Pt nanocrystals. Adapted with permission from ref 88. Copyright 2018 Elsevier.

reduction kinetics revealed that variation of the reduction rates with the concentration of the reductant (Figure 8D) pivotally affected the shape evolution of Pt nanocrystals by changing the ratio between the rates for atom deposition and surface diffusion. At a low concentration of glucose (100 mM), the slow reduction of the Pt(IV) precursor (apparent rate constant $k' = 2.87 \times 10^{-5}$ s^{-1}) allowed atoms that have been deposited onto the seeds enough time for diffusion across the surface, giving rise to thermodynamically favored octahedra as the final product. In contrast, the reduction kinetics was greatly accelerated ($k' = 4.83 \times 10^{-5}$ s^{-1}) when the concentration of glucose was increased to 167 mM. Thus, the deposition of atoms overwhelmed their diffusion on the surface of seeds. In this case, newly formed Pt atoms selectively deposited and piled up on the corners and edges of the cubic seeds because of the high surface energy of these sites, leading to the formation of concave cubes covered by high-index facets. In another report, the reduction kinetics of a Pt(II) precursor at different temperatures was quantitatively analyzed.[89] After the generation of Pt seeds via homogeneous nucleation, the growth of seeds was dominated by surface reduction of the Pt(II) precursor at a low reaction temperature (22 °C), resulting in the formation of large assemblies of Pt nanocrystals. When the reaction temperature was increased to 100 °C, the essentially accelerated reduction kinetics favored reduction of the precursor in the solution phase and thus generated assemblies of Pt nanocrystals with smaller sizes. This trend was also observed in the seed-mediated growth of Pt nanocrystals with Pd cubes serving as seeds.[89] In particular, the switch from surface to solution reduction for the Pt(II) precursor as the reaction temperature increased was similar to the observation in the case of Pd.[36] Recent studies on the preparation of Rh nanocrystals have also stressed the significance of controlling the reduction kinetics in obtaining products with distinctive shapes in a deterministic manner.[90,91] Although the synthetic protocols for different noble-metal nanocrystals may vary from one to another, our mechanistic understanding of the correlation between the reduction kinetics and the resultant Pd nanocrystals can be potentially extended to other metals, guiding their synthesis in a more well-controlled manner. More endeavors are still needed to quantitatively analyze the kinetic parameters of these systems, expanding the applicable scope of the methodology as stated above.

Despite progress in the controllable synthesis of metal nanocrystals by manipulation of the reduction kinetics, there are also challenges that remain to be addressed. First, as discussed in section 5, speciation of the precursor has a profound impact on the reduction kinetics, while limited studies have been conducted on it so far, probably owing to the need for advanced instruments to characterize the chemical species. Second, it is particularly challenging to quantify, interpret, and control the kinetics of reactions involving multiple steps, such as the reduction of high-valent metal precursors, because of the coexistence of metal ions in different valences.[76] The kinetic studies, in turn, can also help to determine the actual intermediates involved in the reaction path.[92] With the combination of advanced characterization techniques and computational studies, it is expected that our understanding in such cases could move ahead. Third, the discovery and specific design of suitable reductants, precursors, or ligands could possibly offer additional knobs for more precise control over the reduction kinetics and thus the outcome of a synthesis. As the synthetic capabilities step forward, noble-metal nanocrystals could be rationally engineered with desired shapes, structures, and properties for practical applications.

Moreover, although the initial reduction rate can be approximated to the rate for nucleation, analysis of the surface growth and diffusion rates of metal atoms and their roles in affecting the shapes of the final products remains largely qualitative. Detailed calculations differentiating the nucleation and growth rates based on the appropriate models are still lacking. In the future, more numerical results of the growth and diffusion rates and a more quantitative understanding of their relationship with the products are desired, enabling us to synthesize metal nanocrystals in a more mechanistically rigorous route. Considering all of the challenges listed above, it should be pointed out that, in the current stage, a "trial-and-error" approach relying on empirical knowledge still shows its great necessity. It is hoped that this Viewpoint could inspire more efforts into the study on colloidal synthesis of noble-metal nanocrystals with quantitative measure, ultimately achieving deterministic and predictable synthetic strategies and outcomes.

AUTHOR INFORMATION

Corresponding Author

Younan Xia − *School of Chemistry and Biochemistry and School of Chemical and Biomolecular Engineering, Georgia Institute of Technology, Atlanta, Georgia 30332, United States; The Wallace H. Coulter Department of Biomedical Engineering, Georgia Institute of Technology and Emory*

https://dx.doi.org/10.1021/acs.inorgchem.0c03576
Inorg. Chem. 2021, 60, 4182−4197

University, Atlanta, Georgia 30332, United States; orcid.org/0000-0003-2431-7048; Email: younan.xia@bme.gatech.edu

Authors

Quynh N. Nguyen − *School of Chemistry and Biochemistry, Georgia Institute of Technology, Atlanta, Georgia 30332, United States;* orcid.org/0000-0003-1544-6139

Ruhui Chen − *School of Chemistry and Biochemistry, Georgia Institute of Technology, Atlanta, Georgia 30332, United States*

Zhiheng Lyu − *School of Chemistry and Biochemistry, Georgia Institute of Technology, Atlanta, Georgia 30332, United States;* orcid.org/0000-0002-1343-4057

Complete contact information is available at: https://pubs.acs.org/10.1021/acs.inorgchem.0c03576

Author Contributions

†Q.N., R.C., and Z.L. contributed equally to the preparation of this paper.

Notes

The authors declare no competing financial interest.

Biographies

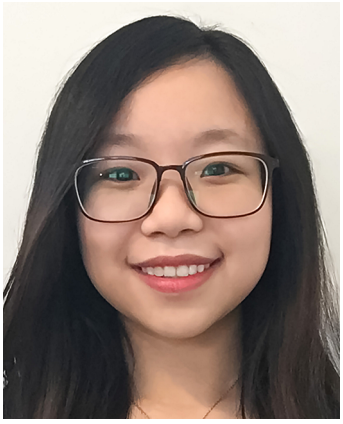

Quynh N. Nguyen received her B.S. in Chemistry from Agnes Scott College in 2020. She is pursuing her Ph.D. at the School of Chemistry and Biochemistry at the Georgia Institute of Technology under the supervision of Prof. Xia. Her research interest includes the shape-controlled synthesis of metal nanocrystals for catalysis and energy-related applications.

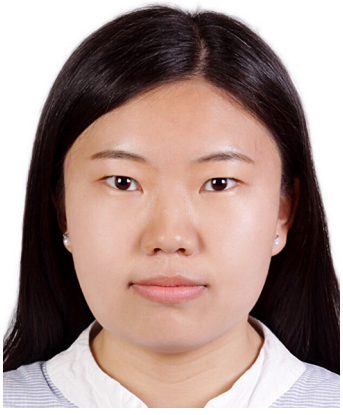

Ruhui Chen received her B.E. in Macromolecular Materials and Engineering from the University of Science and Technology of China in 2017. She is pursuing her Ph.D. in the School of Chemistry and Biochemistry at the Georgia Institute of Technology under the supervision of Prof. Xia. Her research focuses on the development of new methods for controlling the nucleation and growth of nanostructured materials.

Zhiheng Lyu received her B.S. in Chemistry from the University of Science and Technology of China in 2016. She just completed her Ph.D. study under the supervision of Prof. Xia in the School of Chemistry and Biochemistry at the Georgia Institute of Technology. Her research interest includes the shape-controlled synthesis of metal nanocrystals for catalysis and energy-related applications.

Younan Xia received his Ph.D. in Physical Chemistry from Harvard University in 1996 (with George M. Whitesides). He started as an Assistant Professor of Chemistry at the University of Washington—Seattle in 1997 and then joined the Department of Biomedical Engineering at Washington University in St. Louis, MO, in 2007 as the James M. McKelvey Professor. Since 2012, he has held the position of Brock Family Chair and GRA Eminent Scholar in Nanomedicine at the Georgia Institute of Technology. He served as an Associate Editor of *Nano Letters* from 2002 to 2019.

■ ACKNOWLEDGMENTS

This work was supported, in part, by the National Science Foundation (Grants CHE-1804970, CHE-1505441, and DMR-1505400) and startup funds from the Georgia Institute of Technology. We thank our collaborators for their invaluable contributions to these studies.

■ REFERENCES

(1) Talapin, D. V.; Lee, J. S.; Kovalenko, M. V.; Shevchenko, E. V. Prospects of Colloidal Nanocrystals for Electronic and Optoelectronic Applications. *Chem. Rev.* **2010**, *110*, 389−458.

(2) Ye, S.; Rathmell, A. R.; Chen, Z.; Stewart, I. E.; Wiley, B. J. Metal Nanowire Networks: The next Generation of Transparent Conductors. *Adv. Mater.* **2014**, *26*, 6670−6687.

(3) Kauranen, M.; Zayats, A. V. Nonlinear Plasmonics. *Nat. Photonics* **2012**, *6*, 737−748.
(4) Koenderink, A. F.; Alù, A.; Polman, A. Nanophotonics: Shrinking Light-Based Technology. *Science* **2015**, *348*, 516−521.
(5) Liu, L.; Corma, A. Metal Catalysts for Heterogeneous Catalysis: From Single Atoms to Nanoclusters and Nanoparticles. *Chem. Rev.* **2018**, *118*, 4981−5079.
(6) Chen, J.; Lim, B.; Lee, E. P.; Xia, Y. Shape-Controlled Synthesis of Platinum Nanocrystals for Catalytic and Electrocatalytic Applications. *Nano Today* **2009**, *4*, 81−95.
(7) Shi, Y.; Lyu, Z.; Zhao, M.; Chen, R.; Nguyen, Q. N.; Xia, Y. Noble-Metal Nanocrystals with Controlled Shapes for Catalytic and Electrocatalytic Applications. *Chem. Rev.* **2021**, *121*, 649−735.
(8) Alivisatos, P. The Use of Nanocrystals in Biological Detection. *Nat. Biotechnol.* **2004**, *22*, 47−52.
(9) Yang, X.; Yang, M.; Pang, B.; Vara, M.; Xia, Y. Gold Nanomaterials at Work in Biomedicine. *Chem. Rev.* **2015**, *115*, 10410−10488.
(10) Dreaden, E. C.; Alkilany, A. M.; Huang, X.; Murphy, C. J.; El-Sayed, M. A. The Golden Age: Gold Nanoparticles for Biomedicine. *Chem. Soc. Rev.* **2012**, *41*, 2740−2779.
(11) Xia, Y.; Xiong, Y.; Lim, B.; Skrabalak, S. E. Shape-Controlled Synthesis of Metal Nanocrystals: Simple Chemistry Meets Complex Physics? *Angew. Chem., Int. Ed.* **2009**, *48*, 60−103.
(12) An, K.; Somorjai, G. A. Size and Shape Control of Metal Nanoparticles for Reaction Selectivity in Catalysis. *ChemCatChem* **2012**, *4*, 1512−1524.
(13) Xie, S.; Choi, S., Il; Xia, X.; Xia, Y. Catalysis on Faceted Noble-Metal Nanocrystals: Both Shape and Size Matter. *Curr. Opin. Chem. Eng.* **2013**, *2*, 142−150.
(14) Guo, S.; Zhang, S.; Sun, S. Tuning Nanoparticle Catalysis for the Oxygen Reduction Reaction. *Angew. Chem., Int. Ed.* **2013**, *52*, 8526−8544.
(15) Choi, S., Il; Herron, J. A.; Scaranto, J.; Huang, H.; Wang, Y.; Xia, X.; Lv, T.; Park, J.; Peng, H. C.; Mavrikakis, M.; Xia, Y. A Comprehensive Study of Formic Acid Oxidation on Palladium Nanocrystals with Different Types of Facets and Twin Defects. *ChemCatChem* **2015**, *7*, 2077−2084.
(16) Bratlie, K. M.; Lee, H.; Komvopoulos, K.; Yang, P.; Somorjai, G. A. Platinum Nanoparticle Shape Effects on Benzene Hydrogenation Selectivity. *Nano Lett.* **2007**, *7*, 3097−3101.
(17) Bratlie, K. M.; Kliewer, C. J.; Somorjai, G. A. Structure Effects of Benzene Hydrogenation Studied with Sum Frequency Generation Vibrational Spectroscopy and Kinetics on Pt(111) and Pt(100) Single-Crystal Surfaces. *J. Phys. Chem. B* **2006**, *110*, 17925−17930.
(18) Li, D.; Wang, C.; Strmcnik, D. S.; Tripkovic, D. V.; Sun, X.; Kang, Y.; Chi, M.; Snyder, J. D.; Van Der Vliet, D.; Tsai, Y.; Stamenkovic, V. R.; Sun, S.; Markovic, N. M. Functional Links between Pt Single Crystal Morphology and Nanoparticles with Different Size and Shape: The Oxygen Reduction Reaction Case. *Energy Environ. Sci.* **2014**, *7*, 4061−4069.
(19) Dai, Y.; Lu, P.; Cao, Z.; Campbell, C. T.; Xia, Y. The Physical Chemistry and Materials Science behind Sinter-Resistant Catalysts. *Chem. Soc. Rev.* **2018**, *47*, 4314−4331.
(20) Ahmadi, T. S.; Wang, Z. L.; Green, T. C.; Henglein, A.; El-Sayed, M. A. Shape-Controlled Synthesis of Colloidal Platinum Nanoparticles. *Science* **1996**, *272*, 1924−1926.
(21) Burda, C.; Chen, X.; Narayanan, R.; El-Sayed, M. A. Chemistry and Properties of Nanocrystals of Different Shapes. *Chem. Rev.* **2005**, *105*, 1025−1102.
(22) Watzky, M. A.; Finke, R. G. Nanocluster Size-Control and "Magic Number" Investigations. Experimental Tests of the "Living-Metal Polymer" Concept and of Mechanism-Based Size-Control Predictions Leading to the Syntheses of Iridium(0) Nanoclusters Centering about Four Sequential Magic Numbers. *Chem. Mater.* **1997**, *9*, 3083−3095.
(23) Xia, Y.; Xia, X.; Peng, H. C. Shape-Controlled Synthesis of Colloidal Metal Nanocrystals: Thermodynamic versus Kinetic Products. *J. Am. Chem. Soc.* **2015**, *137*, 7947−7966.
(24) Lamer, V. K.; Dinegar, R. H. Theory, Production and Mechanism of Formation of Monodispersed Hydrosols. *J. Am. Chem. Soc.* **1950**, *72*, 4847−4854.
(25) Gilroy, K. D.; Peng, H. C.; Yang, X.; Ruditskiy, A.; Xia, Y. Symmetry Breaking during Nanocrystal Growth. *Chem. Commun.* **2017**, *53*, 4530−4541.
(26) Wang, Y.; He, J.; Liu, C.; Chong, W. H.; Chen, H. Thermodynamics versus Kinetics in Nanosynthesis. *Angew. Chem., Int. Ed.* **2015**, *54*, 2022−2051.
(27) Doye, J. P. K.; Wales, D. J. Global Minima for Transition Metal Clusters Described by Sutton-Chen Potentials. *New J. Chem.* **1998**, *22*, 733−744.
(28) Yang, T. H.; Shi, Y.; Janssen, A.; Xia, Y. Surface Capping Agents and Their Roles in Shape-Controlled Synthesis of Colloidal Metal Nanocrystals. *Angew. Chem., Int. Ed.* **2020**, *59*, 15378−15401.
(29) Loh, N. D.; Sen, S.; Bosman, M.; Tan, S. F.; Zhong, J.; Nijhuis, C. A.; Král, P.; Matsudaira, P.; Mirsaidov, U. Multistep Nucleation of Nanocrystals in Aqueous Solution. *Nat. Chem.* **2017**, *9*, 77−82.
(30) Jin, B.; Wang, Y.; Liu, Z.; France-Lanord, A.; Grossman, J. C.; Jin, C.; Tang, R. Revealing the Cluster-Cloud and Its Role in Nanocrystallization. *Adv. Mater.* **2019**, *31*, 1808225.
(31) Yao, T.; Sun, Z.; Li, Y.; Pan, Z.; Wei, H.; Xie, Y.; Nomura, M.; Niwa, Y.; Yan, W.; Wu, Z.; Jiang, Y.; Liu, Q.; Wei, S. Insights into Initial Kinetic Nucleation of Gold Nanocrystals. *J. Am. Chem. Soc.* **2010**, *132*, 7696−7701.
(32) Yang, J.; Koo, J.; Kim, S.; Jeon, S.; Choi, B. K.; Kwon, S.; Kim, J.; Kim, B. H.; Lee, W. C.; Lee, W. B.; Lee, H.; Hyeon, T.; Ercius, P.; Park, J. Amorphous-Phase-Mediated Crystallization of Ni Nanocrystals Revealed by High-Resolution Liquid-Phase Electron Microscopy. *J. Am. Chem. Soc.* **2019**, *141*, 763−768.
(33) Yang, T. H.; Gilroy, K. D.; Xia, Y. Reduction Rate as a Quantitative Knob for Achieving Deterministic Synthesis of Colloidal Metal Nanocrystals. *Chem. Sci.* **2017**, *8*, 6730−6749.
(34) Watzky, M. A.; Finke, R. G. Transition Metal Nanocluster Formation Kinetic and Mechanistic Studies. A New Mechanism When Hydrogen Is the Reductant: Slow, Continuous Nucleation and Fast Autocatalytic Surface Growth. *J. Am. Chem. Soc.* **1997**, *119*, 10382−10400.
(35) Yin, X.; Shi, M.; Wu, J.; Pan, Y. T.; Gray, D. L.; Bertke, J. A.; Yang, H. Quantitative Analysis of Different Formation Modes of Platinum Nanocrystals Controlled by Ligand Chemistry. *Nano Lett.* **2017**, *17*, 6146−6150.
(36) Yang, T. H.; Peng, H. C.; Zhou, S.; Lee, C. T.; Bao, S.; Lee, Y. H.; Wu, J. M.; Xia, Y. Toward a Quantitative Understanding of the Reduction Pathways of a Salt Precursor in the Synthesis of Metal Nanocrystals. *Nano Lett.* **2017**, *17*, 334−340.
(37) Wang, Y.; Peng, H. C.; Liu, J.; Huang, C. Z.; Xia, Y. Use of Reduction Rate as a Quantitative Knob for Controlling the Twin Structure and Shape of Palladium Nanocrystals. *Nano Lett.* **2015**, *15*, 1445−1450.
(38) Rodrigues, T. S.; Zhao, M.; Yang, T. H.; Gilroy, K. D.; da Silva, A. G. M.; Camargo, P. H. C.; Xia, Y. Synthesis of Colloidal Metal Nanocrystals: A Comprehensive Review on the Reductants. *Chem. - Eur. J.* **2018**, *24*, 16944−16963.
(39) Handwerk, D. R.; Shipman, P. D.; Whitehead, C. B.; Özkar, S.; Finke, R. G. Mechanism-Enabled Population Balance Modeling of Particle Formation En Route to Particle Average Size and Size Distribution Understanding and Control. *J. Am. Chem. Soc.* **2019**, *141*, 15827−15839.
(40) Handwerk, D. R.; Shipman, P. D.; Whitehead, C. B.; Özkar, S.; Finke, R. G. Particle Size Distributions via Mechanism-Enabled Population Balance Modeling. *J. Phys. Chem. C* **2020**, *124*, 4852−4880.
(41) Barnard, A. S.; Young, N. P.; Kirkland, A. I.; Van Huis, M. A.; Xu, H. Nanogold: A Quantitative Phase Map. *ACS Nano* **2009**, *3*, 1431−1436.
(42) Ruditskiy, A.; Zhao, M.; Gilroy, K. D.; Vara, M.; Xia, Y. Toward a Quantitative Understanding of the Sulfate-Mediated Synthesis of Pd

https://dx.doi.org/10.1021/acs.inorgchem.0c03576
Inorg. Chem. 2021, 60, 4182−4197

Decahedral Nanocrystals with High Conversion and Morphology Yields. *Chem. Mater.* **2016**, *28*, 8800−8806.
(43) Huang, H.; Wang, Y.; Ruditskiy, A.; Peng, H. C.; Zhao, X.; Zhang, L.; Liu, J.; Ye, Z.; Xia, Y. Polyol Syntheses of Palladium Decahedra and Icosahedra as Pure Samples by Maneuvering the Reaction Kinetics with Additives. *ACS Nano* **2014**, *8*, 7041−7050.
(44) Huo, D.; Kim, M. J.; Lyu, Z.; Shi, Y.; Wiley, B. J.; Xia, Y. One-Dimensional Metal Nanostructures: From Colloidal Syntheses to Applications. *Chem. Rev.* **2019**, *119*, 8972−9073.
(45) Huang, H.; Zhang, L.; Lv, T.; Ruditskiy, A.; Liu, J.; Ye, Z.; Xia, Y. Five-Fold Twinned Pd Nanorods and Their Use as Templates for the Synthesis of Bimetallic or Hollow Nanostructures. *ChemNanoMat* **2015**, *1*, 246−252.
(46) Huang, H.; Ruditskiy, A.; Choi, S.-I.; Zhang, L.; Liu, J.; Ye, Z.; Xia, Y. One-Pot Synthesis of Penta-Twinned Palladium Nanowires and Their Enhanced Electrocatalytic Properties. *ACS Appl. Mater. Interfaces* **2017**, *9*, 31203−31212.
(47) Xiong, Y.; Siekkinen, A. R.; Wang, J.; Yin, Y.; Kim, M. J.; Xia, Y. Synthesis of Silver Nanoplates at High Yields by Slowing down the Polyol Reduction of Silver Nitrate with Polyacrylamide. *J. Mater. Chem.* **2007**, *17*, 2600−2602.
(48) Figueroa-Cosme, L.; Hood, Z. D.; Gilroy, K. D.; Xia, Y. A Facile, Robust and Scalable Method for the Synthesis of Pd Nanoplates with Hydroxylamine as a Reducing Agent and Mechanistic Insights from Kinetic Analysis. *J. Mater. Chem. C* **2018**, *6*, 4677−4682.
(49) Washio, I.; Xiong, Y.; Yin, Y.; Xia, Y. Reduction by the End Groups of Poly(vinyl pyrrolidone): A New and Versatile Route to the Kinetically Controlled Synthesis of Ag Triangular Nanoplates. *Adv. Mater.* **2006**, *18*, 1745−1749.
(50) Xiong, Y.; Washio, I.; Chen, J.; Cai, H.; Li, Z. Y.; Xia, Y. Poly(vinyl pyrrolidone): A Dual Functional Reductant and Stabilizer for the Facile Synthesis of Noble Metal Nanoplates in Aqueous Solutions. *Langmuir* **2006**, *22*, 8563−8570.
(51) Woehl, T. J. Metal Nanocrystal Formation during Liquid Phase Transmission Electron Microscopy: Thermodynamics and Kinetics of Precursor Conversion, Nucleation, and Growth. *Chem. Mater.* **2020**, *32*, 7569−7581.
(52) Özkar, S.; Finke, R. G. Dust Effects on Nucleation Kinetics and Nanoparticle Product Size Distributions: Illustrative Case Study of a Prototype $Ir(0)_n$ Transition-Metal Nanoparticle Formation System. *Langmuir* **2017**, *33*, 6550−6562.
(53) Handwerk, D. R.; Shipman, P. D.; Özkar, S.; Finke, R. G. Dust Effects on $Ir(0)_n$ Nanoparticle Formation Nucleation and Growth Kinetics and Particle Size-Distributions: Analysis by and Insights from Mechanism-Enabled Population Balance Modeling. *Langmuir* **2020**, *36*, 1496−1506.
(54) Özkar, S.; Finke, R. G. A Classic Azo-Dye Agglomeration System: Evidence for Slow, Continuous Nucleation, Autocatalytic Agglomerative Growth, Plus the Effects of Dust Removal by Microfiltration on the Kinetics. *J. Phys. Chem. A* **2017**, *121*, 7071−7078.
(55) Yang, T. H.; Zhou, S.; Gilroy, K. D.; Figueroa-Cosme, L.; Lee, Y. H.; Wu, J. M.; Xia, Y. Autocatalytic Surface Reduction and Its Role in Controlling Seed-Mediated Growth of Colloidal Metal Nanocrystals. *Proc. Natl. Acad. Sci. U. S. A.* **2017**, *114*, 13619−13624.
(56) El-Sayed, M. A. Small Is Different: Shape-, Size-, and Composition-Dependent Properties of Some Colloidal Semiconductor Nanocrystals. *Acc. Chem. Res.* **2004**, *37*, 326−333.
(57) Van Hardeveld, R.; Hartog, F. The Statistics of Surface Atoms and Surface Sites on Metal Crystals. *Surf. Sci.* **1969**, *15*, 189−230.
(58) Vara, M.; Xia, Y. Facile Synthesis of Pd Concave Nanocubes: From Kinetics to Mechanistic Understanding and Rationally Designed Protocol. *Nano Res.* **2018**, *11*, 3122−3131.
(59) Su, N.; Chen, X.; Yue, B.; He, H. Formation of Palladium Concave Nanocrystals via Auto-Catalytic Tip Overgrowth by Interplay of Reduction Kinetics, Concentration Gradient and Surface Diffusion. *Nanoscale* **2016**, *8*, 8673−8680.
(60) Figueroa-Cosme, L.; Gilroy, K. D.; Yang, T. H.; Vara, M.; Park, J.; Bao, S.; da Silva, A. G. M.; Xia, Y. Synthesis of Palladium Nanoscale Octahedra through a One-Pot, Dual-Reductant Route and Kinetic Analysis. *Chem. - Eur. J.* **2018**, *24*, 6133−6139.
(61) Lyu, Z.; Xie, M.; Gilroy, K. D.; Hood, Z. D.; Zhao, M.; Zhou, S.; Liu, J.; Xia, Y. A Rationally Designed Route to the One-Pot Synthesis of Right Bipyramidal Nanocrystals of Copper. *Chem. Mater.* **2018**, *30*, 6469−6477.
(62) Wang, Y.; Xie, S.; Liu, J.; Park, J.; Huang, C. Z.; Xia, Y. Shape-Controlled Synthesis of Palladium Nanocrystals: A Mechanistic Understanding of the Evolution from Octahedrons to Tetrahedrons. *Nano Lett.* **2013**, *13*, 2276−2281.
(63) Zhu, C.; Zeng, J.; Tao, J.; Johnson, M. C.; Schmidt-Krey, I.; Blubaugh, L.; Zhu, Y.; Gu, Z.; Xia, Y. Kinetically Controlled Overgrowth of Ag or Au on Pd Nanocrystal Seeds: From Hybrid Dimers to Nonconcentric and Concentric Bimetallic Nanocrystals. *J. Am. Chem. Soc.* **2012**, *134*, 15822−15831.
(64) Kang, S. W.; Lee, Y. W.; Park, Y.; Choi, B. S.; Hong, J. W.; Park, K. H.; Han, S. W. One-Pot Synthesis of Trimetallic Au@PdPt Core-Shell Nanoparticles with High Catalytic Performance. *ACS Nano* **2013**, *7*, 7945−7955.
(65) Lee, Y. W.; Kim, M.; Kim, Z. H.; Han, S. W. One-Step Synthesis of Au@Pd Core-Shell Nanooctahedron. *J. Am. Chem. Soc.* **2009**, *131*, 17036−17037.
(66) Wang, L.; Yamauchi, Y. Autoprogrammed Synthesis of Triple-Layered Au@Pd@Pt Core-Shell Nanoparticles Consisting of a Au@Pd Bimetallic Core and Nanoporous Pt Shell. *J. Am. Chem. Soc.* **2010**, *132*, 13636−13638.
(67) Ortiz, N.; Weiner, R. G.; Skrabalak, S. E. Ligand-Controlled Co-Reduction versus Electroless Co-Deposition: Synthesis of Nanodendrites with Spatially Defined Bimetallic Distributions. *ACS Nano* **2014**, *8*, 12461−12467.
(68) Zhou, M.; Wang, H.; Vara, M.; Hood, Z. D.; Luo, M.; Yang, T. H.; Bao, S.; Chi, M.; Xiao, P.; Zhang, Y.; Xia, Y. Quantitative Analysis of the Reduction Kinetics Responsible for the One-Pot Synthesis of Pd-Pt Bimetallic Nanocrystals with Different Structures. *J. Am. Chem. Soc.* **2016**, *138*, 12263−12270.
(69) Feldberg, S.; Klotz, P.; Newman, L. Computer Evaluation of Equilibrium Constants from Spectrophotometric Data. *Inorg. Chem.* **1972**, *11*, 2860−2865.
(70) Wang, X.-B.; Wang, L.-S. Photodetachment of Multiply Charged Anions: The Electronic Structure of Gaseous Square-Planar Transition Metal Complexes PtX_4^{2-} (X = Cl, Br). *J. Am. Chem. Soc.* **2000**, *122*, 2339−2345.
(71) Zhou, M.; Wang, H.; Elnabawy, A. O.; Hood, Z. D.; Chi, M.; Xiao, P.; Zhang, Y.; Mavrikakis, M.; Xia, Y. Facile One-Pot Synthesis of $Pd@Pt_{1L}$ Octahedra with Enhanced Activity and Durability toward Oxygen Reduction. *Chem. Mater.* **2019**, *31*, 1370−1380.
(72) Lee, C. T.; Wang, H.; Zhao, M.; Yang, T. H.; Vara, M.; Xia, Y. One-Pot Synthesis of $Pd@Pt_{nL}$ Core-Shell Icosahedral Nanocrystals in High Throughput through a Quantitative Analysis of the Reduction Kinetics. *Chem. - Eur. J.* **2019**, *25*, 5322−5329.
(73) Yang, T. H.; Zhou, S.; Zhao, M.; Xia, Y. Quantitative Analysis of the Multiple Roles Played by Halide Ions in Controlling the Growth Patterns of Palladium Nanocrystals. *ChemNanoMat* **2020**, *6*, 576−588.
(74) Niu, Z.; Peng, Q.; Gong, M.; Rong, H.; Li, Y. Oleylamine-Mediated Shape Evolution of Palladium Nanocrystals. *Angew. Chem., Int. Ed.* **2011**, *50*, 6315−6319.
(75) Xie, M.; Lyu, Z.; Chen, R.; Xia, Y. A Mechanistic Study of the Multiple Roles of Oleic Acid in the Oil-Phase Synthesis of Pt Nanocrystals. *Chem. - Eur. J.* **2020**, *26*, 15636−15642.
(76) Chen, S.; Yang, Q.; Wang, H.; Zhang, S.; Li, J.; Wang, Y.; Chu, W.; Ye, Q.; Song, L. Initial Reaction Mechanism of Platinum Nanoparticle in Methanol-Water System and the Anomalous Catalytic Effect of Water. *Nano Lett.* **2015**, *15*, 5961−5968.
(77) Strach, M.; Mantella, V.; Pankhurst, J. R.; Iyengar, P.; Loiudice, A.; Das, S.; Corminboeuf, C.; Van Beek, W.; Buonsanti, R. Insights into Reaction Intermediates to Predict Synthetic Pathways for Shape-

https://dx.doi.org/10.1021/acs.inorgchem.0c03576
Inorg. Chem. 2021, 60, 4182−4197

Controlled Metal Nanocrystals. *J. Am. Chem. Soc.* **2019**, *141*, 16312−16322.
(78) Zhang, H.; Jin, M.; Wang, J.; Li, W.; Camargo, P. H. C.; Kim, M. J.; Yang, D.; Xie, Z.; Xia, Y. Synthesis of Pd-Pt Bimetallic Nanocrystals with a Concave Structure through a Bromide-Induced Galvanic Replacement Reaction. *J. Am. Chem. Soc.* **2011**, *133*, 6078−6089.
(79) Xie, M.; Zhou, S.; Zhu, J.; Lyu, Z.; Chen, R.; Xia, Y. A Quantitative Analysis of the Reduction Kinetics Involved in the Synthesis of Au@Pd Concave Nanocubes. *Chem. - Eur. J.* **2019**, *25*, 16397−16404.
(80) Kriek, R. J.; Mahlamvana, F. Dependency on Chloride Concentration and "in-Sphere" Oxidation of H 2O for the Effective TiO 2-Photocatalysed Electron Transfer from H_2O to $[PdCl_n(H_2O)_{4-n}]^{2-n}$ (n = 0−4) in the Absence of an Added Sacrificial Reducing Agent. *Appl. Catal., A* **2012**, *423*−*424*, 28−33.
(81) le Roux, C. J.; Kriek, R. J. A Detailed Spectrophotometric Investigation of the Complexation of Palladium(II) with Chloride and Bromide. *Hydrometallurgy* **2017**, *169*, 447−455.
(82) Mozaffari, S.; Li, W.; Thompson, C.; Ivanov, S.; Seifert, S.; Lee, B.; Kovarik, L.; Karim, A. M. Colloidal Nanoparticle Size Control: Experimental and Kinetic Modeling Investigation of the Ligand-Metal Binding Role in Controlling the Nucleation and Growth Kinetics. *Nanoscale* **2017**, *9*, 13772−13785.
(83) Zhou, S.; Mesina, D. S.; Organt, M. A.; Yang, T. H.; Yang, X.; Huo, D.; Zhao, M.; Xia, Y. Site-Selective Growth of Ag Nanocubes for Sharpening Their Corners and Edges, Followed by Elongation into Nanobars through Symmetry Reduction. *J. Mater. Chem. C* **2018**, *6*, 1384.
(84) Özkar, S.; Finke, R. G. Nanoparticle Nucleation Is Termolecular in Metal and Involves Hydrogen: Evidence for a Kinetically Effective Nucleus of Three $\{Ir_3H_{2x}{\cdot}P_2W_{15}Nb_3O_{62}\}^{6-}$ in $Ir(0)_n$ Nanoparticle Formation From $[(1,5\text{-COD})Ir^{I}{\cdot}P_2W_{15}Nb_3O_{62}]^{8-}$ Plus Dihydrogen. *J. Am. Chem. Soc.* **2017**, *139*, 5444−5457.
(85) Whitehead, C. B.; Finke, R. G. Nucleation Kinetics and Molecular Mechanism in Transition-Metal Nanoparticle Formation: The Intriguing, Informative Case of a Bimetallic Precursor, $\{[(1,5\text{-COD})Ir^{I}{\cdot}HPO_4]_2\}^{2-}$. *Chem. Mater.* **2019**, *31*, 2848−2862.
(86) Su, D. Advanced Electron Microscopy Characterization of Nanomaterials for Catalysis. *Green Energy Environ.* **2017**, *2*, 70−83.
(87) Shi, Y.; Lyu, Z.; Cao, Z.; Xie, M.; Xia, Y. How to Remove the Capping Agent from Pd Nanocubes without Destructing Their Surface Structure for the Maximization of Catalytic Activity? *Angew. Chem., Int. Ed.* **2020**, *59*, 19129−19135.
(88) Qian, J.; Shen, M.; Zhou, S.; Lee, C. T.; Zhao, M.; Lyu, Z.; Hood, Z. D.; Vara, M.; Gilroy, K. D.; Wang, K.; Xia, Y. Synthesis of Pt Nanocrystals with Different Shapes Using the Same Protocol to Optimize Their Catalytic Activity toward Oxygen Reduction. *Mater. Today* **2018**, *21*, 834−844.
(89) Zhou, S.; Yang, T. H.; Zhao, M.; Xia, Y. Quantitative Analysis of the Reduction Kinetics of a Pt(II) Precursor in the Context of Pt Nanocrystal Synthesis. *Chin. J. Chem. Phys.* **2018**, *31*, 370−374.
(90) Zhang, N.; Shao, Q.; Pi, Y.; Guo, J.; Huang, X. Solvent-Mediated Shape Tuning of Well-Defined Rhodium Nanocrystals for Efficient Electrochemical Water Splitting. *Chem. Mater.* **2017**, *29*, 5009−5015.
(91) Choi, S.-I.; Lee, S. R.; Ma, C.; Oliy, B.; Luo, M.; Chi, M.; Xia, Y. Facile Synthesis of Rhodium Icosahedra with Controlled Sizes up to 12 nm. *ChemNanoMat* **2016**, *2*, 61−66.
(92) Whitehead, C. B.; Özkar, S.; Finke, R. G. LaMer's 1950 Model of Particle Formation: A Review and Critical Analysis of Its Classical Nucleation and Fluctuation Theory Basis, of Competing Models and Mechanisms for Phase-Changes and Particle Formation, and then of Its Application to Silver Halide, Semiconductor, Metal, and Metal-Oxide Nanoparticles. *Mater. Adv.* **2021**, *2*, 186.

https://dx.doi.org/10.1021/acs.inorgchem.0c03576
Inorg. Chem. 2021, 60, 4182−4197